Use Authorization

In presenting this dissertation in partial fulfillment of the requirements for an advanced degree of PhD in Engineering and Applied Science at Idaho State University, I agree that the Library shall make it freely available for inspection. I further state that permission to download and/or print my dissertation for scholarly purposes may be granted by the Dean of the Graduate School, Dean of my academic division, or by the University Librarian. It is understood that any copying or publication of this dissertation for financial gain shall not be allowed without my written permission.

Signature: ________________________________

Date: ____________________________________

SIMULATION and REAL-TIME CONTROL of a SMART PROSTHETIC HAND

by

Amir Fassih

A dissertation

submitted in partial fulfillment

of the requirements for the degree of

Doctor of Philosophy in the Engineering & Applied Science

Idaho State University

December 2013

To the Graduate Faculty:

The members of the committee appointed to examine the dissertation of AMIR FASSIH find it satisfactory and recommend that it be accepted.

____ Major Advisor

Dr. D. Subbaram Naidu (Professor of Electrical Engineering)

____ Co- Advisor

Dr. Steve C. Chiu, (Associate Professor of Electrical Engineering)

______________________________________ Committee Member

Dr. Marco P. Schoen, (Professor of Mechanical Engineering)

_______________________________________ Committee Member

Dr. Yuriy Gryazin (Associate Professor of Mathematics)

____________________________ Graduate Faculty Representative

Dr. Jim Creelman (Associate Professor of Physical Therapy)

ACKNOWLEDGEMENTS

In completion of the research work for my PhD, there are several individuals who were of great help. I feel very humble and privileged to have their support for this work. For the technical aspects of this work, I would like to express my gratitude to my Major advisor **Dr. Subbaram Naidu** and Co-Adviser **Dr. Steve Chiu** for their help and guidance. At the same time, I appreciate the help and support of the other members of my dissertation committee, Dr. Marco Schoen and Dr. Yuriy Gryazin. I also appreciate the help and co-operation of other graduate, undergraduate students, and office staff at School of Engineering, College of Science and Engineering, Idaho State University. The financial support of the US Department of the Army, under the award number W81XWH-10-1-0128 awarded and administered by the U.S. Army Medical Research Acquisition Activity, 820 Chandler Street, Fort Detrick MD 21702-5014 is greatly appreciated.

Table of Contents

List of Figures

List of Tables

List of Publications

- Amir Fassih, D.Subbaram Naidu, Steve Chiu, Parmod Kumar, "Robust Control of a Prosthetic Hand Based on a Hybrid Adaptive Finger Angle Estimation", WSEAS Conf. Athen, Greece, March 7-9,2012
- Amir Fassih, D.Subbaram Naidu, Steve Chiu, Parmod Kumar, "Design and Control of an Underactuated Prosthetic Hand", Wseas Conf. Athen, Greece, March 7-9,2012
- Fassih, D.S. Naidu, S. Chiu, And M.P. Schoen, "Power Grasping of a Prosthetic Hand Based Upon Virtual Spring-Damper Hypothesis", IASTED Int. Conf. Robotics And Applications, Cambridge, MA, November 1 – 3, 2010
- Fassih, D.S. Naidu, S. Chiu, And M.P. Schoen, "Precision Grasping of a Prosthetic Hand Based on Virtual Spring Damper Hypothesis", Ieee 5th Cairo International Biomedical Engineering Conference, Cairo, Egypt, Dec 2010
- P. Kumar, C. H. Chen, A. Sebastian, M. Anugolu, C. Potluri, A. Fassih, Y. Yihun, A. Jensen, Y. Tang, S. Chiu, K. Bosworth, "An Adaptive Hybrid Data Fusion Based Identification of Skeletal Muscle Force With Anfis And Smoothing Spline Curve Fitting", International Conference On Fuzzy Systems, Taipei, Taiwan, June 27 - June 30, 2011.

Abstract

In this research different strategies for controlling a smart prosthetic hand are investigated. The aim of the controller is to provide a signal for movement of fingers considering the amputee's intention and an appropriate grasp shape. Two major kinds of plants are covered: fully actuated and underactuated hands. In fully actuated hands all the joints of the fingers are active and they have separate actuators, while in an underactuated hand the number of actuators is less than degrees of freedom. Besides grasp formation strategies, control techniques that allow accurately following command signal from EMG analysis in real-time are investigated. These commands can be in the form of position (angle) or force signals. All the purposed control strategies are designed for real-time implementation.

1.INTRODUCTION TO PROSTHETIC HAND DESIGN AND CONTROL

The design of fully functioning artificial hand replacement with physiological speed of response and strength that can be controlled almost without thought is the ultimate goal of prosthetic hand researches. Unfortunately, current prosthetic components and interface techniques are still a long way from realizing this goal. The current state-of-the-art prosthesis can be considered to be a tool rather than a limb replacement.

The prosthesis as a tool does not try to replace the lost limb physiologically but there is an aid to help provide some of the functions that were lost. The prosthesis as a tool is an interchangeable device that is worn and used as needed. Much effort in the field of upper-extremity prosthesis research is directed toward the creation of prostheses as true limb replacements; however, in current practice we are mostly limited to prostheses as tools.

The major causes of the limitation of prostheses as tools and not limb replacements are practical ones due to the severe weight, power, and size constraints of hand/arm systems as well as the difficulty in finding a sufficient number of appropriate control sources to control the requisite number of degrees of freedom. Of these, it is the lack of independent control sources that imposes the most severe impediment to the development of today's prosthetic hand systems. As a result, upper limb prosthetics research is somewhat dominated by considerations of control.

1.1. Prosthetic Hand vs. Robotic Hand

The problems associated with the design of artificial hand replacements are far more challenging than those associated with the design of robotic arms or terminal devices. In fact, robotics and prosthetics design has much less in common than one might expect. Robotics concepts have had little impact on commercial prosthetics because of the severe physical constraints required for a prosthetic device to be successful. Although some size, weight, and power constraints must be placed on robots and manipulators, robotic actuators can often be as large and as heavy as required to achieve a specific result. Power is usually not an issue since it can be obtained from the power mains.

Prosthetic hand design can be viewed as a subset of the greater field of robot and manipulator arm and end-effector design. Robot arms look impressive. However robotic hands are not necessarily appropriate as a prosthetic hand. The issue has never been about an inability to build mechanical arms and hands. The MIT/Utah dexterous hand [1] is an example of a mechanical hand that mimics the function of a hand. This hand was designed for use in research studying robot dexterity. This device could never be used in prosthetics because the actuators and computer system required to control this hand are very big, and power is supplied externally from electrical mains. The real issue in upper-limb prosthetics, of which most robot arm designers seem to be unaware, is “How does one interface this arm to the person?” and “How is the arm to be controlled?”

The design of artificial hands is a multidisciplinary endeavor. A designer needs an understanding of the mechanics of mechanisms such as gears, levers, points of mechanical advantage, and electromechanical design such as switches, dc motors, and electronics. In addition to these skills, the prosthesis designer must also have knowledge of musculoskeletal anatomy, and muscularas well as neurophysiology. The relationship of different parts of a prosthetic hand is shown in Figure 1.1.

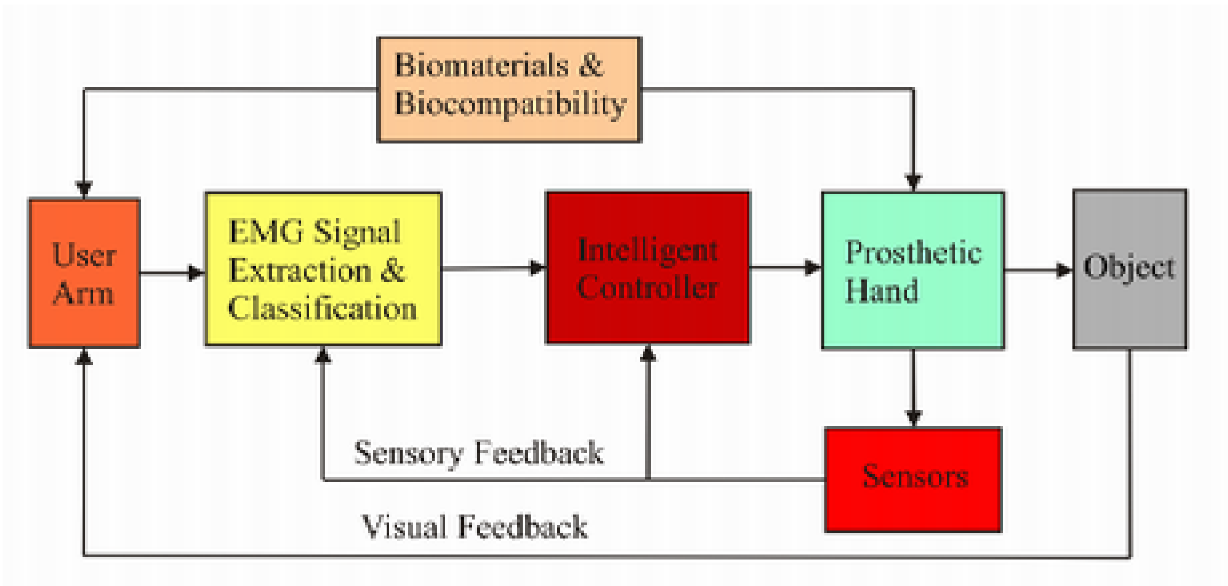

Figure 1.1: Block Diagram of Prosthetic Hand Control Systems

1.2. <u>The Control Challenge</u>

There are over 30 muscles acting on the forearm and hand. The human hand has 27 major bones, and at least 18 joint articulations with 27 or more degrees of freedom (DOF). The arm contributes another 7 degrees of freedom. The primary role of the arm is to position the hand in space. The primary role of the hand is to enable a person to interact with the environment. Control of a person's arm is directed at controlling the position of the arm's hand. Even though people control their arms with great fidelity, this is a highly complex and demanding task.

To have an idea about complexity of hand control problem consider a backhoe which is essentially a mechanical arm that is under the control of an operator. To control this mechanical arm the operator uses both arms, both feet, both eyes, and all of his or her concentration (Figure. 1.2). The driver uses both arms to pull levers, both feet to press pedals to operate the arm, and both eyes to monitor the task being performed by the digger. All these are to control a single mechanical arm. Now consider a person with upper-extremity (e.g., above the elbow) amputations and one begins to have some appreciation of the task such a limbless person faces in controlling a prosthetic hands.

Figure 1.2. A Backhoe made by Caterpillar© Co. To control this mechanical arm the operator uses both arms, both feet, both eyes, and all of his or her concentration.

As for performance, the anatomical hand is capable of speeds in excess of 40 rad/s (2290 degrees/s) and grasps involving all fingers of the hand can exert up to about 400 N of force. Average physiological speeds for everyday pick-and-place tasks have been found to be in the range of 3 to 4 rad/s (172 to 200 degrees/s), while most activities of daily living (ADLs) require prehension forces in the range 0 to 67 N. These forces are dependent on the coefficient of friction between the gripping surface and the object held [2].

Another property of the physiologic hand is that it is compliant or spring-like. This compliance is not a fixed quantity but can be varied, depending on the task requirements: a stiff hand for holding an object a relaxed hand for touching an object.

This inherent compliance of the human arm hand provides protection for the joints and musculoskeletal system. Because the musculoskeletal system is compliant, it can withstand external shock loads far better than can a stiff-jointed equivalent.

Interaction with the real world is something current robotics and prosthetics actuators (dc electric motors with gear trains) do not do well. When a stiff robot arm comes into contact with a hard surface, a phenomenon, known as *contact instability*, can arise unless the robot satisfies certain passivity requirements [3].

The performance of current artificial mechanisms comes nowhere close to meeting the maximum speed and force of which the anatomic arm and hand are capable, although hand mechanisms are available [4] that can attain speeds in excess of 3 rad/s and pinch forces in excess of 110 N. The Otto Bock Wrist Rotator is the only commercially available electric wrist rotator. It is slow (1rad/s) and produces minimal torque. Motion Control is set to release a much faster and stronger wrist rotator which is integrated into the hand, and Otto Bock is working on a faster and stronger wrist rotator as well. All other prosthetic wrist components are body-powered and, when used, are used for positioning purposes.

Current electric-powered prosthetic elbows can attain up to 18 N/m of “live-lift” (lift by the elbows’ own motor mechanism) and speeds of up to 4 rad/s [5].

Body-powered elbows are limited by the speed and strength of the user and the efficiency of the linkage used to connect the user and the component. Humeral rotation for elbow components, with the exception of the RIMJET body-powered humeral rotator [6], is achieved with manually positioned friction joints or turntables. The only shoulder joints available are also passive, manually positioned units that use friction or a lock to hold their position.

Thus it is apparent that, although the user-prosthesis interface is a major impediment to the advancement of prosthetic technology, there is much room for improvement in the prosthetic components themselves. The limitations of current systems are not due to a lack of innovative design but rather due to the very severe nature of the physical constraints that are placed on the designer and the inability of current technology to match the power density of natural muscle.

1.3. Prehension or Grasp

Hand function is generally limited to those modes of prehension that are used the most often. Numerous studies of how the hands grasp objects have been performed [7,8,9,10]. Broadly speaking, hand tasks can be subdivided into nonprehensile functions and prehensile functions. Nonprehensile functions of the hand are those functions where grasping is not required; for example, pushing an object, holding an object between the body and forearm, flicking, brushing, percussive motions such as playing the piano, and so on. Prehensile hand functions are those cases where an object is grasped and held partly or wholly within the hand. The 6 grasping patterns adapted by Keller et al. [8] from Schlesinger et al.'s [7] 12 patterns are the most widely accepted in the field of prosthetics (Fig. 1.3) and have endured the test of time. These patterns are

- Tip prehension
- Palmar prehension
- Lateral prehension
- Hook prehension
- Spherical prehension
- Cylindrical prehension

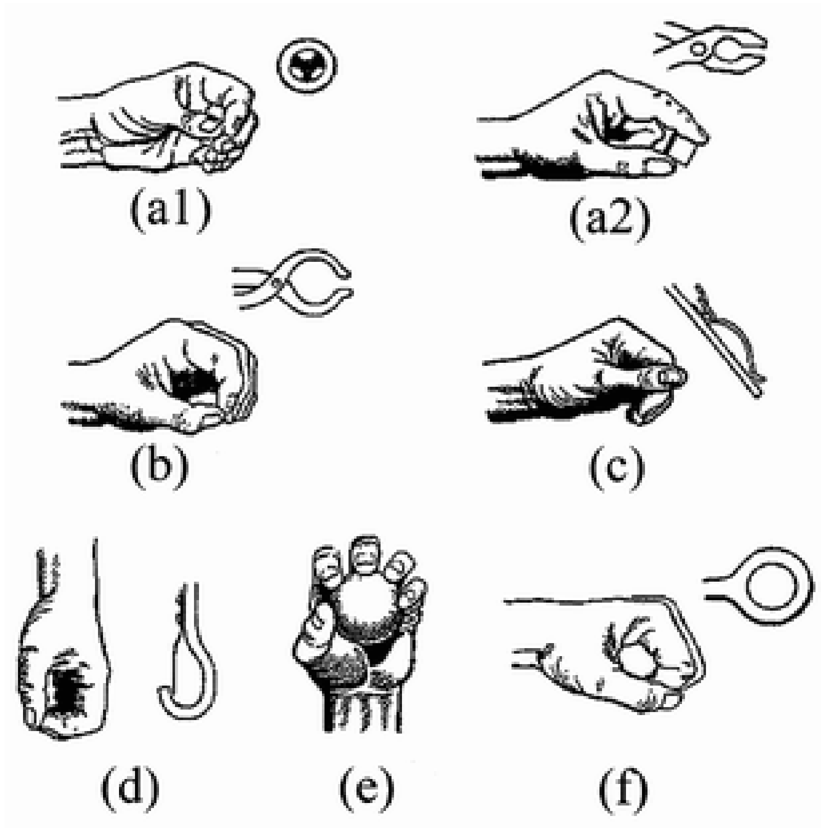

Figure 1.3 Schematic of the prehension patterns of the hand as defined by Keller et al. (1947): (*a*1) palmar prehension (three jaw chuck), (*a*2) palmar prehension (two finger), (*b*) tip prehension, (*c*) lateral prehension, (*d*) hook prehension, (*e*) spherical prehension, (*f*) cylindrical prehension. In a hand-like prosthesis, it takes two to four independently controlled degrees of freedom to implement these prehension patterns. In a non-hand-like device, a single degree-of-freedom device such as a split hook can be used.

Napier [9] described tip prehension, palmar prehension, and lateral prehension as precision grips and spherical and cylindrical prehension as power grasp, while hook prehension falls outside of both these categories. Precision grips primarily involve the thumb working in opposition with the index and middle fingers. Tip prehension, or fingernail pinch, is used mainly to grasp small objects. In lateral prehension, the thumb holds an object against the side of the index finger as is the case when using a key. In palmar prehension (sometimes referred to as tridigital pinch or three-jaw chuck), the thumb opposes either a single finger or two or more fingers.

Power grasps use all the fingers of the hand to provide an encompassing grasp that firmly stabilizes the object being held. Hook prehension is achieved by flexing the fingers into a hook; the thumb is either alongside the index finger or opposes the index and middle fingers to lock the object held.

Carrying a briefcase is a good illustration of this kind of prehension. Keller et al. [8] found that palmar prehension or tridigital pinch was the most frequently used prehensile pattern for static grasping, while lateral prehension is used most often for dynamic grasping.

The finding by Keller et al. [8] that palmar prehension was the most frequently used pattern and the reduction of most prosthetic terminal devices to a single DOF has meant that most prosthetic terminal devices incorporate palmar prehension as the dominant grasp pattern. The persistence of this pattern combined with a wide width of opening in prosthetic hand designs and its general acceptance over the years tend to support this compromise (Heckathorne, [11]).

A study done at the University of California, Los Angeles (UCLA), by Taylor [12] on human prehension force indicated that adult males could produce maximum mean forces of 95.6 N of palmar prehension, 103 N for lateral prehension, and 400 N for cylindrical grasp. In the light of another, unpublished, UCLA study that showed forces up to 68N were needed for carrying out activities of daily living, Peizer et al. [13] proposed that 68N be a minimum standard for the maximum prehension force for electric prehensors (Heckathorne, [11]).

Most manipulations of the hand are precision manipulations of the palmar prehension kind where the thumb directly opposes the index finger and/or the middle finger. In this mode, most of the hand's actions are performed with a hand opening of about 5 cm (2 in) (Keller et al., [8]). When designing for dominant hand function, palmar prehension is the desirable pattern with emphasis not so much on wide opening. For nondominant hand function where the hand is used essentially as a portable vice with objects being placed into it, a wide opening becomes more important.

From a design perspective, allowing the hand mechanism to open 10 cm (3.5 to 4 in), instead of 5 cm (2 in) enables the mechanism to perform the cylindrical prehension power grasp with minimal extra design effort. In general, an artificial hand should be able to open at least 10 cm (3.5 to 4 in), or enough to grasp a beverage can or a Mason jar, which are common household items.

1.4. Passive Adaptation During Grasping.

The grip of the hand is improved by the ability of the hand to passively adapt to the shape of an object grasped. A grasped object depresses, or indents, the skin and underlying soft tissues of the hand, at first meeting little reaction. Consequently, the soft tissue adapts easily to the shape of the object grasped. However, the mechanical properties of the soft tissue are nonlinear, and the conforming tissue becomes more rigid as pressure is increased. The rise in tissue stiffness after conformation to shape enables objects to be grasped securely. This feature of the human hand would seem to be useful for robotic and prosthetic systems. In prosthetics, the passive adaptability, afforded by the soft tissue of the hand, is mimicked, to some extent, by lining the prosthesis mechanism with a soft plastic and covering it with a cosmetic glove. In robotics, it is common to use a compliant coating on an end effector to stabilize a robot arm during contact with hard surfaces.

1.5. Non-Hand-Like Prehensors

The reduction of most prosthetic terminal devices to a single degree of freedom (DOF) was a compromise to make the best use of the available control sources. A standard transhumeral (above-elbow) body-powered prosthesis has two control cables (two active DOF). The terminal device invariably takes the form of a split hook. A split hook is used when maximum function is desired (Fig. 1.4).

Fig 1.4. Non-Hand-Like Prehensors

Although a split hook is a single DOF device, depending on which part of the hook is used, a split hook can reproduce tip, palmar, lateral, cylindrical, or hook prehension, making it a very simple and versatile device. This is another contributing factor to the success of body-powered prostheses over externally powered prostheses.

The use of split hooks highlights the tradeoff made between form and function. The hook bears little resemblance to the natural hand but is widely used because of the function it affords if only one DOF is available for terminal device control. Split hooks are available in many variations on a basic theme from Hosmer-Dorrance Corp. and Otto Bock Healthcare.

1.6. Hand-Like Prehensors

The standard for externally powered hand-like prosthesis is the single DOF Otto Bock Sensor Hand Speed (Fig. 1.5).When used in a prosthetic fitting, a plastic hand form liner is pulled over the mechanism and a PVC or silicone rubber cosmetic glove is then pulled over the liner. This gives the hand good overall *static* cosmesis at the expense of reduced overall mechanism performance. RSLSteeper Ltd. (Roehampton, England) and Centri (Sweden) also manufacture single DOF devices for the adult. Single DOF child-size hands are also available from Systemteknik, Variety Village, Otto Bock Orthopaedic Inc., and RSLSteeper Ltd., among others.

Fig 1.5 DOF Otto Bock Sensor Hand Speed

Touch Bionics has recently introduced the i-Limb Hand, in which each finger has a separate motor. This prosthetic hand is able to easily conform around objects, since each finger continues to flex until it meets resistance. The position of the thumb may be manually adjusted, providing palmer prehension or lateral prehension. Whether this hand will prove robust enough remains to be seen. The liner and cosmetic glove act as springs to oppose the opening of the hand by the mechanism, thus degrading the overall performance of the hand. De Visser and Herder [14] advocated the use of compensatory mechanisms to reduce the effect of the liner and glove on the mechanisms' performance.

Palmar prehension, in these hand-like prehensors, is achieved by single joint fingers that are fixed in slight flexion at a position approximating the interphalangeal joint. The resulting finger shape also creates a concave inner prehension surface that can be used to provide cylindrical prehension [15].

All these mechanisms are typically used in a prosthesis that has no wrist flexion or extension. This can be a problem when trying to pick up small objects from a surface. The fixed wrist combined with poor line of sight of the object to be grasped can lead to nonphysiological movements, resulting in poor *dynamic* cosmesis.

1.7. Control Sources

1.7.1. Body-Powered Control

Body-powered control has been described above as a suitable energy source to power prostheses. It is also a good control source. Although friction in the cable limits the fidelity of force transmission or sensation, the coupling of a proximal joint to the distal prosthesis provides a good proprioceptive link, which in turn decreases the cognitive burden on the user. Body powered control may be used without visual feedback, and with a moderate degree of certainty regarding the position and exerted force of the terminal device. The largest impediment to bodypowered control is that there are a very limited number of joints which may be coupled to the artificial limb without impeding other functions. As a result, conventionally body-powered control may only be used to control single DOF at a time, precluding the use of multifunctional prostheses.

Ironically, it is the area of multifunctional prostheses, where the high mental load of coordinating multiple DOFs is significant, where the proprioceptive feedback of body-powered control would otherwise excel. Body-powered control may be used to control a single DOF, and as such may be part of a hybrid multifunctional prosthesis.

1.7.2. Myoelectric Control.

Myoelectric control derives its name from the Latin word for muscle (*myo*) and the resulting by-product of electricity that muscle contraction creates. It is commonly called *electromyographic (EMG) control*, although strictly speaking *electromyography* refers to the recording of myoelectric signals, rather than to the actual signals themselves. When a muscle contracts, an electric potential is produced as a by-product of that contraction. If surface electrodes are placed on the skin near a muscle, they can detect this signal (Fig. 1.6). The signal can then be electronically amplified, processed, and used to control prosthesis. Although the intensity of the EMG increases as muscle tension increases, the relationship is a complex nonlinear process that is dependent on many variables, including the position and configuration of the electrodes [16]. Although the EMG is nonlinear, it is broadly monotonic, and the human operator perceives this response as more or less linear.

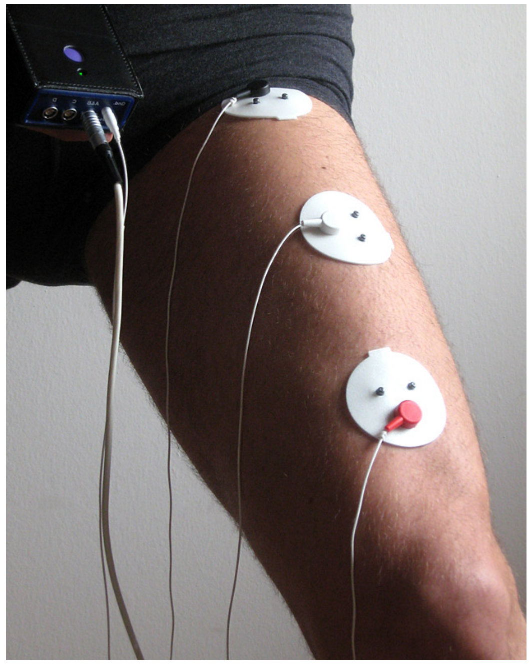

Fig 1.6. The EMG Electrodes Placed on Skin

The first externally powered prosthesis was a pneumatic hand patented in Germany in 1915. Drawings of this hand and possibly the first electric hand were published in 1919 in *Ersatzgliederund Arbeitshilfen* [17]. The first myoelectric prosthesis was developed during the early 1940s by Reinhold Reiter. He published his work in 1948 [18] but it was not widely known, and myoelectric control had to wait to be rediscovered during the 1950s. Reiter's prosthesis consisted of a modified Hüfner hand that contained a control electromagnet controlled by a vacuum tube amplifier. The prosthesis was not portable but was instead intended for use at a workstation, although Reiter did hope that one day it might be portable. The Russian hand was the first semipractical myoelectric hand to be used clinically. This hand also had the distinction of being the first to use transistors (germanium) to process the myoelectric control signal [19].

Myoelectric control has received considerable attention since it first appeared during the 1940s, and there is an extensive body of literature on myoelectric characteristics and properties [20, 21]. It was considered to be the cutting edge of technology of the day and was advanced as a natural approach for the control of prostheses since it made it possible for amputees to use the same mental processes to control prosthesis function as had previously been used in controlling their physiological limb [22, 23].

Usually, the EMG is amplified and processed (bandlimited, rectified, and thresholded) to provide a dc signal that is related to the force of muscular contraction; this is then used to control the prosthesis. EMG processing in a typical prosthetic myoelectric control system involves two pairs of differential "dry" metal electrodes and a reference electrode (Fig. 1.7).

Fig 1.7. EMG Sensor

Although the electrodes are referred to as dry, the environment inside a prosthetic socket causes the amputee's residual limb to sweat, which creates a conductive interface between the skin and the electrodes. As a result, performance typically improves 5 min or so after donning the prosthesis. Traditionally, myoelectric control uses electrodes placed on the skin near each of a protagonist/antagonist pair of muscles to control a single DOF. For below-elbow fittings, this usually means electrodes on those muscle groups responsible for flexion and extension of the wrist and fingers. Thinking about flexing or extending the "phantom" fingers controls closing or opening, respectively, of some terminal device.

EMG signal amplitude is approximately 100 μV for a moderately contracted forearm muscle. This signal must be amplified to a signal with an amplitude in the range of 1 to 10 V before it can used. This implies that a gain of upward of 10,000 is needed. The bandwidth for the surface EMG signals is 10 to 300 Hz with most of the signals' energy in and around 100 Hz [24].

Differential amplifiers are used to amplify the EMG because the small EMG signal is often superimposed on large common mode signals that, at these gain levels, would saturate an amplifier in a single-mode configuration. A differential amplifier can remove the large common-mode signals, leaving only the potential difference (EMG signal) between the electrodes to be amplified. This has the effect of most effectively amplifying the EMG signal frequencies around 100 Hz. Because the large gain requirement would drive most op-amps to instability, these differential amplifiers are seldom single op-amps, but instead use multiple stages to meet the gain requirements.

Once the EMG signal has been amplified and bandlimited, it is then changed into a dc signal. This dc potential is then commonly smoothed with a low-pass filter to remove the pulses and extract the envelope of the signal. For on/off, or switch, control, the smoothed dc voltage, is then compared in a logic circuit with a threshold voltage. If the signal is greater than the threshold voltage, then power is supplied to the prosthesis motor, otherwise the power remains off. For proportional control, the smoothed voltage is fed to the motor.

When used for proportional control, the EMG signal is usually treated as an amplitude-modulated signal, where the mean amplitude of the cutaneous signal is the desired output from the myoelectric processor. However, in order to have accurate estimates of muscle force from EMG signals, a processing system with high signal-to-noise ratio (SNR) as well as short rise time (fast response) is required [25]. Unfortunately, there is a fundamental filtering paradox whereby it is possible to have either fast response or high SNR, but not both [26]. To overcome this perceived problem, Meek et al. [27] proposed using an adaptive filter in which the time constant of the low-pass filter used in the final stage of EMG processing (acquire signal envelope) was varied, depending on the rate of change of the EMG signal. Their assumption was that an amputee, when moving quickly, will tolerate noise (low SNR) but will not tolerate delays in control. When holding the prosthesis steady or performing slow, dexterous tasks such as treading a needle, the amputee will tolerate slow response as long as there is low noise (high SNR).

Designers need to be aware of this filtering paradox should they be involved in the design of high bandwidth, myoelectrically controlled systems. It is also questionable whether the user needs an accurate measure of muscle force versus EMG signal amplitude. So long as the control signal is broadly monotonic, the user learns to equate a particular level of contraction with a particular control signal output.

Finally, all these processing steps take time! Any delay in the response of the output to a change in the input of greater than 250 μs is perceptible to the human operator as a “sluggish” response. Any delay at all decreases functional performance, and a delay greater than 100 μs creates clinically significant reduction in performance [28].

2.POWER GRASPING CONTROL FOR FULLY ACTUATED PROSTHETIC HAND

2.1. Introduction

Human hand is one of the most important and complex parts of the body, which has the ability to handle different tasks. The ultimate goal of a robotic hand is to achieve the functionality of a human hand. In the past three decades, there have been numerous investigations to achieve dexterity and ability of human hand, especially in the fields of humanoid robotics and prosthetic hand [1-6]. In spite of all these advances in this field, the current state of research on prosthetic hands is far from that objective of achieving the functionality of human hand. Commercially available prosthetic hands have very limited functionality and they are just simple grippers. The present research on prosthetic hands involves complex control schemes to achieve the most important functions of the hand [7-8].

Grasping can be categorized into two main groups: precision and power grasping. In precision grasping the object is held by tips of the fingers, while in power grasping, the whole the finger is active and in contact with the object [9].

Many control methods require the knowledge of the shape of the object. For humans this information is available by visual feedback from eyes, while in case of a prosthetic hand this visual information is not directly available for hand controller, and the only available information is electromyographic (EMG) signal related to patient’s arm muscle activities.

However, normally the EMG signal is not available for all individual joints and besides, due to measurement noise, accessing high quality EMG signal is hard [10]. Moreover, using EMG signal to control all the movements requires lot of attention during grasping and leads to fatigue for the amputees [11]. Hence it is required for prosthetic hand to be semi-autonomous which means a part of command information will be provided by the EMG signal and the rest of the required command should be provided automatically by hand controller.

Defining finger trajectory without the knowledge of shape of object to be grasped is a challenging task for many path planning techniques. For multi DOFs robots there are two common methods for trajectory planning which are "inverse kinematic" and "inverse dynamic" [12-15]. Both these methods require object shape and are based on solving optimization problem which requires high computation, hence they are hard to implement for real-time applications.

To avoid solving the path planning problem for prosthetic hands, many researchers advocated under-actuated mechanisms, which are capable of adapting to object shape mechanically and without additional computation [16-18]. In these mechanisms, the number of actuators are less than the DOFs, and because of less actuators they have less weight. However fewer actuators result in less functionality, because fingers joints can't move independently. In this research the control methods for both underactuated and fully actuated hands will be covered.

Arimoto et al. [19] used “virtual spring-damper hypothesis” for control of robotic arm-hand systems. A similar method called “virtual model control” is also suggested by J.Pratt et al. [20] used for walking robots, and it is based on defining virtual forces between two points. Both methods are based on the use of Jacobian matrix to relate task space movement to joint space. In [20] it is shown that any kind of force can be defined between two points and the other study [19] shows that use of spring-damper forces will result in human like movement. From physiological point of view, human skilled multi-joint reaching movement has these characteristics that 1) endpoint trajectory become a quasi-straight line and less variable, 2)velocity profiles of the endpoint has a bell-shape, and 3) joint trajectories are rather variable from trial to trial [19].

In this research, a new control scheme is proposed that can efficiently address the problem of power grasping without complete knowledge of the shape of the object which may be called “blind power grasping” for prosthetic hand. The proposed method is based on the works by Arimoto et al. [19] using virtual spring-damper (VSD) hypothesis used for control of robotic arm-hand systems. In our research, we use the above mentioned hypothesis, in particular for the power grasping of a prosthetic hand. In this method, we define a virtual spring-damper between finger tip and desired point for control of movement of fingers. Further, in this method there is no need to introduce any performance indices to solve inverse kinematics uniquely and Jacobian pseudo-inverse or inverse dynamics which are common methods to define trajectories of redundant DOFs robots. Besides, in the present method, there is no need for any information on tactile or force sensing.

2.2. Modeling of Prosthetic Hand

In this control method, controller is not derived directly from dynamic model of the system. Kinematics equation and Jacobian matrix are the required for controller design.

A model of a robotic hand system is shown in Fig 2.1. The model consists of a finger with 3DOF which represents three joints of a finger and palm.

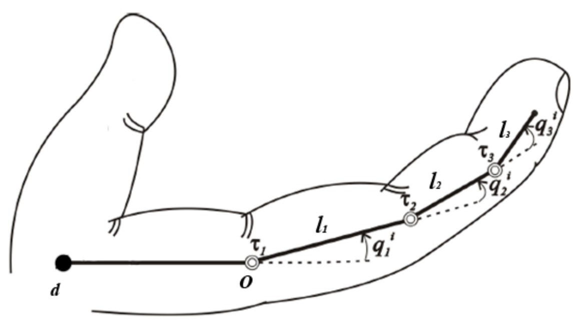

Fig. 2.1 Model of a Robotic Hand System

In this research we assume the following:

1- Movement of both finger and object are confined to a two dimensional horizontal plane, and therefore there is no gravity effect.

2- The object is assumed to be initially stable in its position.

3- The initial movement toward object is handled by amputee, so the hand is close enough to the object before grasping.

The position of the tip of the finger is evaluated as (Fig 2.1):

$$x = l_1 \cos q_1 + l_2 \cos(q_1 + q_2) + l_3 \cos(q_1 + q_2 + q_3) \quad (2\text{-}1)$$

$$y = l_1 \sin q_1 + l_2 \sin(q_1 + q_2) + l_3 \sin(q_1 + q_2 + q_3) \quad (2\text{-}2)$$

where, l_1, l_2, and l_3 are lengths of each finger and q_1, q_2, and q_3 are angles of each corresponding joint.

Based on above equation the Jacobian matrix is as:

$$= \begin{bmatrix} j_{11} & j_{12} & j_{13} \\ j_{21} & j_{22} & j_{23} \end{bmatrix} \; J = \begin{bmatrix} j_{11} & j_{12} & j_{13} \\ j_{21} & j_{22} & j_{23} \end{bmatrix}, \tag{2-3}$$

$$= -l_1 \sin q_1 - l_2 \sin[\![(q]\!]_1 + q_2) - l_3 \ \mathbf{sin}[\![(q]\!]_1 + q_2 + q_3) \tag{2-4}$$
$$= -l_1 \sin q_1 - l_2 \sin[\![(q]\!]_1 + q_2) - l_3 \ \mathbf{sin}[\![(q]\!]_1 + q_2 + q_3)$$

$$= -l_2 \sin[\![(q]\!]_1 + q_2) - l_3 \sin[\![(q]\!]_1 + q_2 + q_3) \tag{2-5}$$
$$= -l_2 \sin[\![(q]\!]_1 + q_2) - l_3 \sin[\![(q]\!]_1 + q_2 + q_3),$$

$$= -l_2 \sin[\![(q]\!]_1 + q_2) - l_3 \sin[\![(q]\!]_1 + q_2 + q_3) \tag{2-6}$$
$$= -l_2 \sin[\![(q]\!]_1 + q_2) - l_3 \sin[\![(q]\!]_1 + q_2 + q_3),$$

$$= -l_3 \sin[\![(q]\!]_1 + q_2 + q_3) j_{13} = -l_3 \sin[\![(q]\!]_1 + q_2 + q_3) \tag{2-7}$$

$$= l_1 \cos q_1 + l_2 \cos[\![(q]\!]_1 + q_2) + l_3 \ \mathbf{cos}[\![(q]\!]_1 + q_2 + q_3)$$
$$= l_1 \cos q_1 + l_2 \cos[\![(q]\!]_1 + q_2) + l_3 \ \mathbf{cos}[\![(q]\!]_1 + q_2 + q_3) \tag{2-8}$$

$$= l_2 \cos[\![(q]\!]_1 + q_2) + l_3 \cos[\![(q]\!]_1 + q_2 + q_3). \tag{2-9}$$

$$= l_3 \cos[\![(q]\!]_1 + q_2 + q_3). \tag{2-10}$$

2.3. Virtual Spring-Damper Method

"Virtual model control" is a motion control scheme that uses simulations of virtual components to generate desired joint torques [20]. These joints produce the same effect that the virtual elements placed on robot would have created; hence they create the illusion that these virtual elements are connected to the real robot. Virtual elements can be any kind of real physical elements such as springs, dampers, gravity fields, nonlinear fields or any other components.

Virtual model control was proposed by J. Pratt et al [20] for biped walking robot. In a study by Arimoto [19] on robotic hand arm system, it is shown that using a virtual spring damper between robot end effector and desired point, and virtual dampers at each joint, human like movement can be achieved.

For power grasping by a prosthetic hand, one of the best options is the use of Virtual Spring-Damper (VSD) hypothesis. Some benefits of VSD control scheme are that it has a simple structure and requires relatively less computation. Besides, it doesn't need inverse dynamics to precisely define the robot movement. Thus, we use spring set points instead of commanded movement and robot automatically adapts its shape. Since finger joints at prosthetic hand work as virtual dampers, which is sensitive to velocity and not to position, they don't have a forced shape, instead just finger tip follow a defined path as will be discussed more in control strategy section.

The joint torques to virtual forces is given by:

$$\tau = J^T F \ \tau = J^T F \ , \qquad (2\text{-}11)$$

where τ is the torque, and *F* is the force due to virtual spring damper given as

$$F = -\left(\xi\sqrt{k}\dot{x} + k\Delta x\right) F = -\left(\xi\sqrt{k}\dot{x} + k\Delta x\right), \qquad (2\text{-}12)$$

and

$$_{damper} = -J^T\left(\xi\sqrt{k}\dot{x} + k\Delta x\right). \tag{2-13}$$

where k represents the stiffness of the virtual spring, Δx is distance between finger tip and desired point, and ξ is the damping ratio. The damping force is defined at each joint as

$$_{damping} = -C\dot{q} \qquad \tau_{joints\ damping} = -C\dot{q} \tag{2-14}$$

,

where, C denotes a diagonal positive definite matrix as follows:

$$iag(c_1, \dots, c_n). \tag{2-15}$$

Hence control signal would be sum of these two terms

$$- J^T(q)(\xi\sqrt{k}\dot{x} + k\Delta x). \tag{2-16}$$

Higher values of k result in more accurate and faster response to the desired point and higher C provides more stability. Thus k and C are chosen as design variables.

2.4. Control Strategy

Virtual spring-damper hypothesis is suitable for point to point control. Defining the desired trajectory as a semicircle (in order to have a full grasp of the object) given by,

$$+ l_3)\cos(t), \tag{2-17}$$

$$+ l_3)\sin(t)\, y_d = (l_1 + l_2 + l_3)\sin(t), \tag{2-18}$$

Where t is proportional to EMG signal which is scaled to change between $0<t<\pi$.

As shown in Fig. 2.2, after passing this semi-circle, finger tip goes toward center to make a tighter grasping. This is achieved by defining a desired point close to center.

As mentioned earlier, the goal is not exactly following the defined path. If the object is big, due to contact of hand and object, it would be impossible to follow exact path and following this path is just to achieve grasping.

Fig. 2.3 illustrates the physical counterparts of the virtual forces for control strategy and Fig. 2.4 shows structure of the proposed control system. As shown, the command force comes from EMG signal, and controller provides the movement for hand which has dynamic interaction with the object.

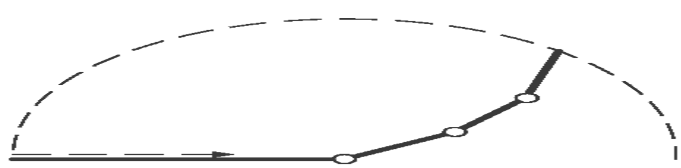

Fig. 2.2: Semi-Circle Path of Finger Tip

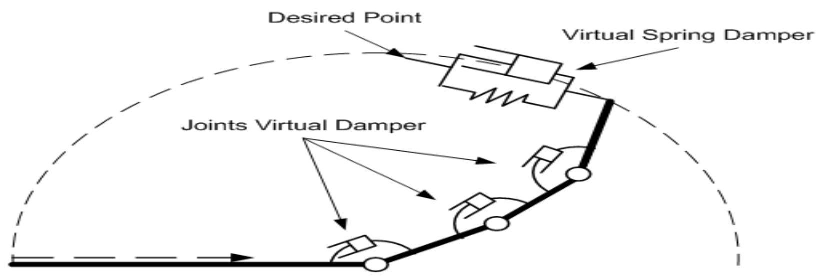

Fig 2.3: Physical Counterparts of the Virtual Forces

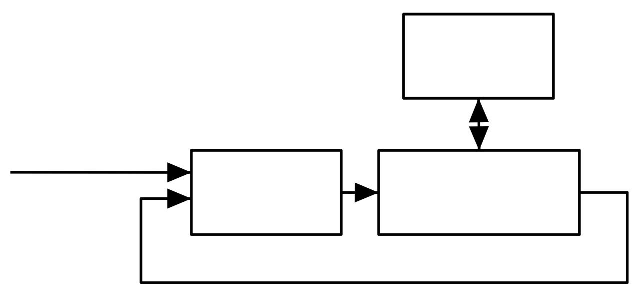

Fig. 2.4: Control Diagram of Prosthetic Hand System

2.5. Numerical Simulation

In order to show the effectiveness of the proposed control strategy, numerical simulations were conducted to grasp three different objects, based on the physical parameters of a hand system and objects summarized in Table 2.1.

In order to simulate dynamics of the hand and interaction with object, Adams software is used. This software is a multi-body analysis simulation program that solves the rigid body dynamic equilibrium equations and directly interfaces with Matlab/Simulink software in order to implement controller. The contact between object and hand is modeled and three sets of simulations with different objects are performed. In all three simulations the same control strategy is used which shows controller can handle grasping without information about physical parameters of object. Fingers and objects are assumed to be rigid. In these simulations the EMG signal is assumed to increase linearly with time.

Table 2.1. Parameters used for simulation

Index finger link 1	5 cm
Index finger link 2	2.5 cm
Index finger link 3	2.5 cm
Damping at joints	0.01 kg/s
Virtual damping ratio *(c)*	1
Virtual spring stiffness *(k)*	50 N/m
Rectangular object width	3 cm
Circular object radius	3 cm
Star shape object outer radius	2 cm

2.6. Simulation One

For first simulation a rectangular (cubic) object is used, and as mentioned earlier the movement is restricted to 2D movement. Object is not moving initially. Hand starts movement from open finger configuration. The hand positions at 1 second time interval are shown. Fig. 2.5 shows finger tip angle with respect to palm.

As it is shown in Fig. 6 the grasping is accomplished successfully.

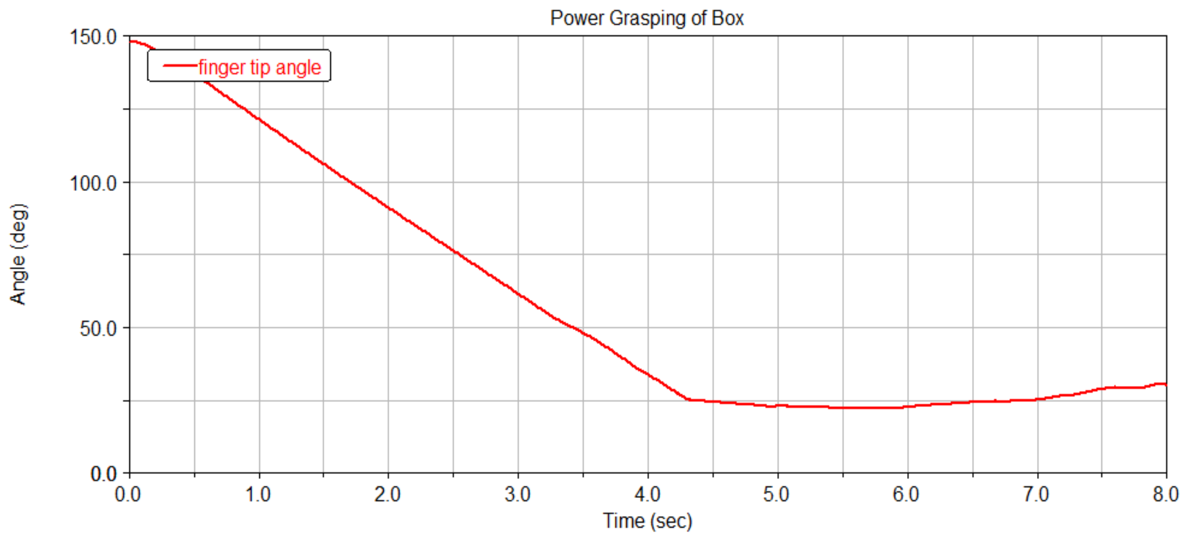

Fig. 2.5: Finger's Tip Angle at Rectangular Object Grasping

2.7. Simulation Two

For the second simulation a glass (circular object) is used. The control parameters are identical to previous simulation.

As shown in Fig. 2.7 the grasping is done successfully and the hand positions for 1 second time interval are depicted. Similarly the finger tip angle respect to palm is shown in Fig. 2.8.

Regardless of object shape, by use of proposed control scheme the hand can successfully grasp objects.

2.8. Simulation Three

For the third simulation a star shape object is used. The control parameters are identical to previous simulation.

As shown in Fig. 2.9 the grasping is done successfully and the hand positions for 1 second time interval are illustrated. Similarly the finger tip angle respect to palm is shown in Fig. 2.10.

The complicated shape of object shows that controller is able to handle grasp for wide variety of objects, without information of object shape.

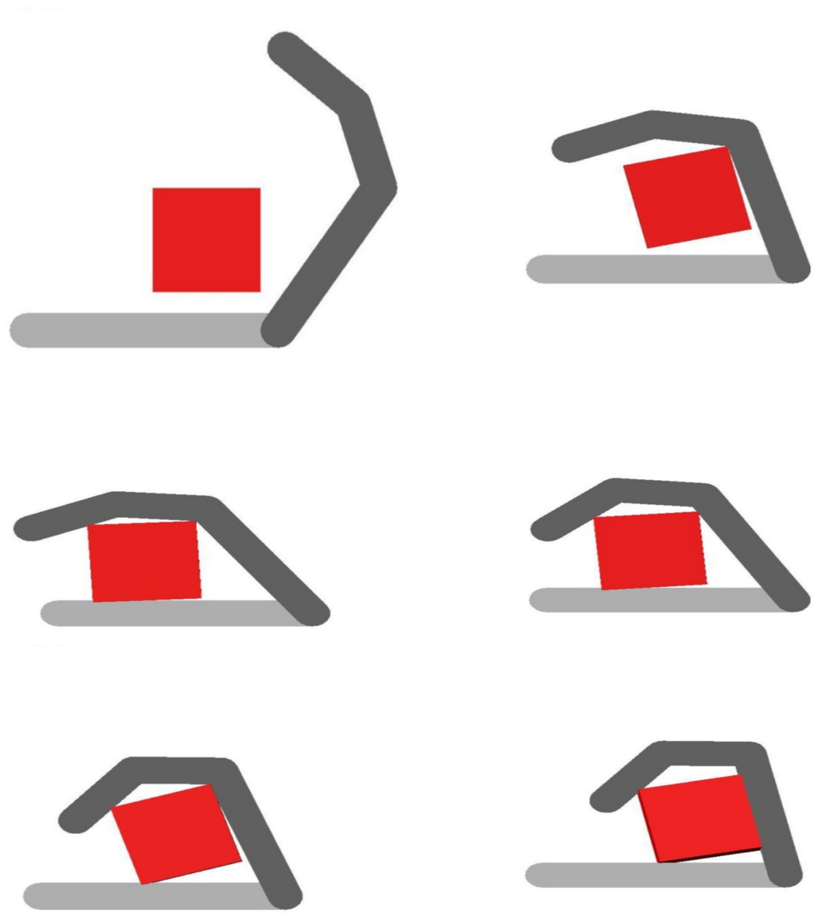

Fig. 2.6: Rectangular Object Grasping

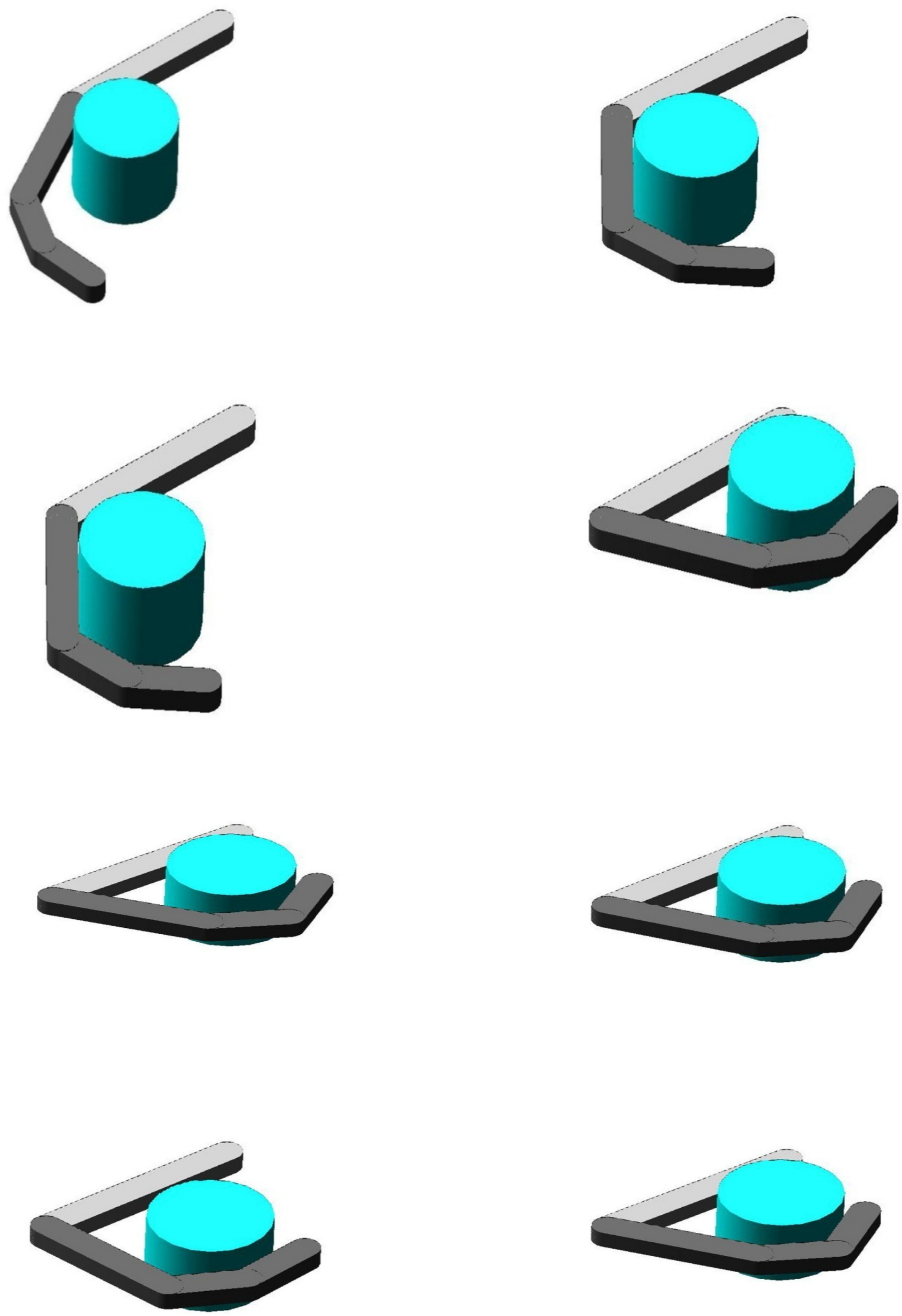

Fig. 2.7 Grasping of a Glass

Fig. 2.8 Grasping of Star Shape Object

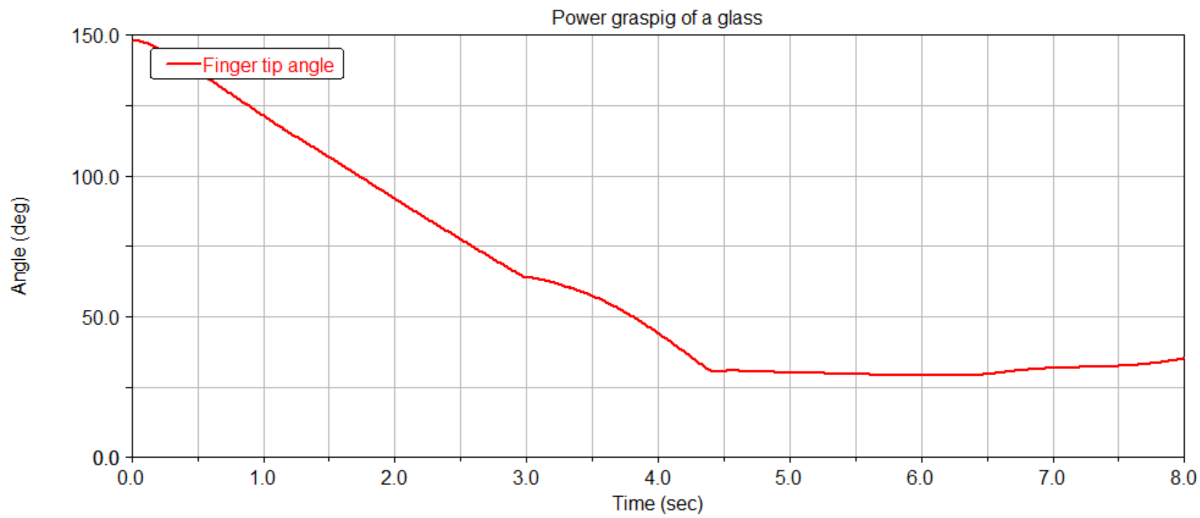

Fig. 2.9: Finger’s Tip Angle at Grasping a Glass

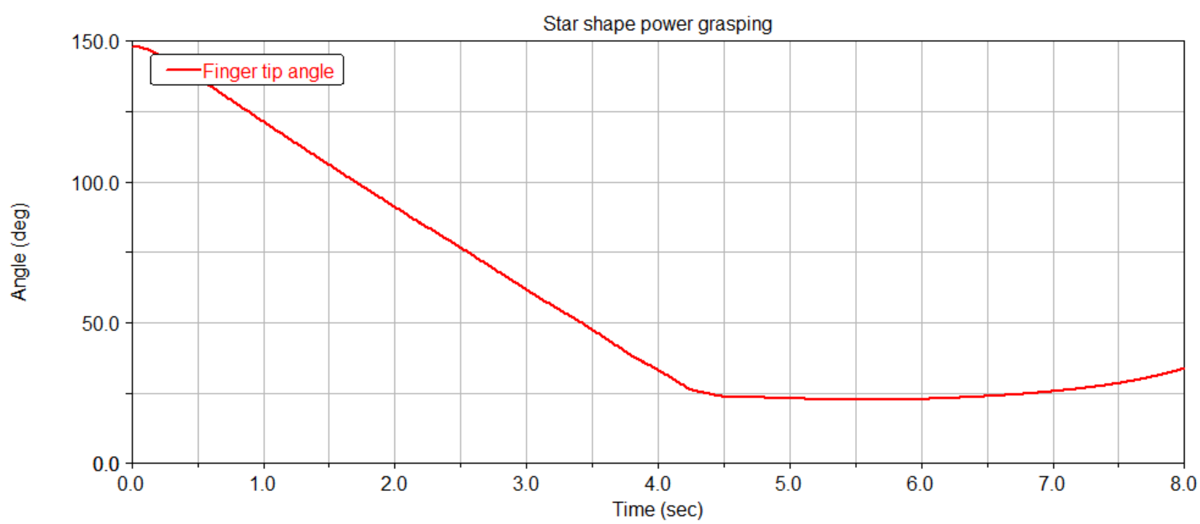

Fig. 2.10: Finger’s Tip Angle at Star Shape Object Grasping

3. Precision grasping control for fully actuated prosthetic hand

Using the similar technique discussed in previous chapter for power grasping which is virtual spring damper hypothesis a control strategy is developed for precision grasping. In precision grasping the object is held by tips of the fingers, while in power grasping, the whole finger is active and in contact with the object. First a model is derived for kinematic of the hand, then the control strategy and numerical simulations are provided.

3.1. Modeling of Prosthetic Hand

In this control method, controller is not designed based on dynamic model of the system. Instead, kinematics equation and Jacobian matrix are used for controller design.

A model of a robotic hand system is shown in Fig.1. The model consists of a finger with 3DOF which represents three joints of index finger, palm and a finger with 2DOF which represents thumb.

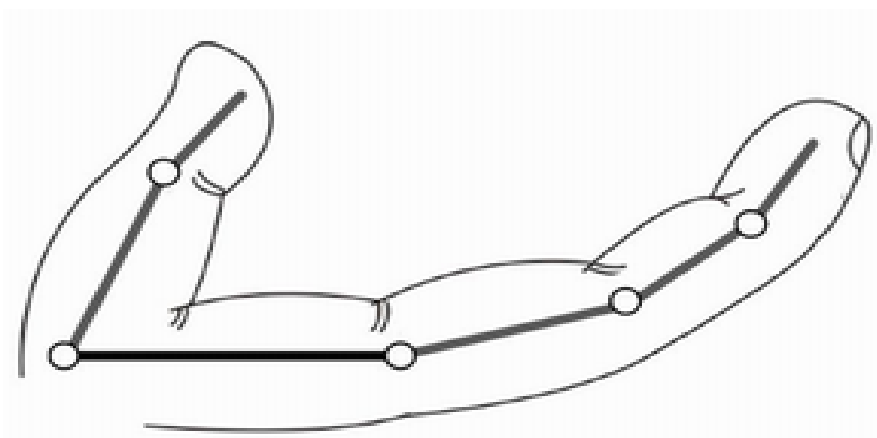

Fig. 3.1. Schematic of a robotic hand system

In this reseach we assume the following:

- Movement of both finger and object are confined to a 2 dimensional horizontal plane, and therefore there is no gravity effect.
- The object is assumed to be initially stable in its position.
- The initial movement toward object is handled by amputee, so the hand is close enough to the object before grasping.

The position of the tip of index fingers is evaluated as (see Fig. 1):

$$x_i = l_{i1} \cos q_{i1} + l_{i2} \cos(q_{i1} + q_{i2}) + l_{i3} \cos(q_{i1} + q_{i2} + q_{i3}),$$

$$x_i = l_{i1} \cos q_{i1} + l_{i2} \cos(q_{i1} + q_{i2}) + l_{i3} \cos(q_{i1} + q_{i2} + q_{i3}), \qquad (3\text{-}1)$$

$$y_i = l_{i1} \sin q_{i1} + l_{i2} \sin(q_{i1} + q_{i2}) + l_{i3} \sin(q_{i1} + q_{i2} + q_{i3})$$

$$y_i = l_{i1} \sin q_{i1} + l_{i2} \sin(q_{i1} + q_{i2}) + l_{i3} \sin(q_{i1} + q_{i2} + q_{i3}), \qquad (3\text{-}2)$$

where, l_{i1}, l_{i2}, and l_{i3} are lengths of index finger and q_{i1}, q_{i2}, and q_{i3} are angles of each corresponding joint. Similarly the position of thumb finger is evaluated as:

$$x_t = l_{t1} \cos q_{t1} + l_{t2} \cos(q_{t1} + q_{t2}), \qquad (3\text{-}3)$$

$$y_t = l_{t1} \sin q_{t1} + l_{t2} \sin(q_{t1} + q_{t2}), \qquad (3\text{-}4)$$

where, l_{t1} and l_{t2} are lengths of thumb finger and q_{t1} and q_{t2}, are angles of corresponding joints.

Based on above equation the Jacobian matrix for index finger is as:

$$J_i = \begin{bmatrix} \frac{\partial x}{\partial q_{i1}} & \frac{\partial x}{\partial q_{i2}} & \frac{\partial x}{\partial q_{i3}} \\ \frac{\partial y}{\partial q_{i1}} & \frac{\partial y}{\partial q_{i2}} & \frac{\partial y}{\partial q_{i3}} \end{bmatrix}, \qquad (3\text{-}5)$$

and Jacobian for thumb finger is as:

$$J_t = \begin{bmatrix} \frac{\partial x}{\partial q_{t1}} & \frac{\partial x}{\partial q_{t2}} \\ \frac{\partial y}{\partial q_{t1}} & \frac{\partial y}{\partial q_{t2}} \end{bmatrix} J_t = \begin{bmatrix} \frac{\partial x}{\partial q_{t1}} & \frac{\partial x}{\partial q_{t2}} \\ \frac{\partial y}{\partial q_{t1}} & \frac{\partial y}{\partial q_{t2}} \end{bmatrix}. \quad (3\text{-}6)$$

3.2. Control Strategy

Virtual spring-damper hypothesis is suitable for point to point control. In precision grasping two approaches can be considered. 1) Defining a virtual spring damper between fingers tip and geometrical center of the object, which requires information about the object position and shape, and this information is not available in case of a prosthetic hand for the controller which is used in [13] 2) Defining a virtual spring damper between tips of two fingers, then fingers attract together and grasp the object in between, without exact knowledge of object position and shape. In this case the amputee should place the hand close to the object and in appropriate position. Besides, a virtual damper force is considered at each finger joint. The latter method is used and physical counterpart of virtual forces are depicted at Fig. 3.2.

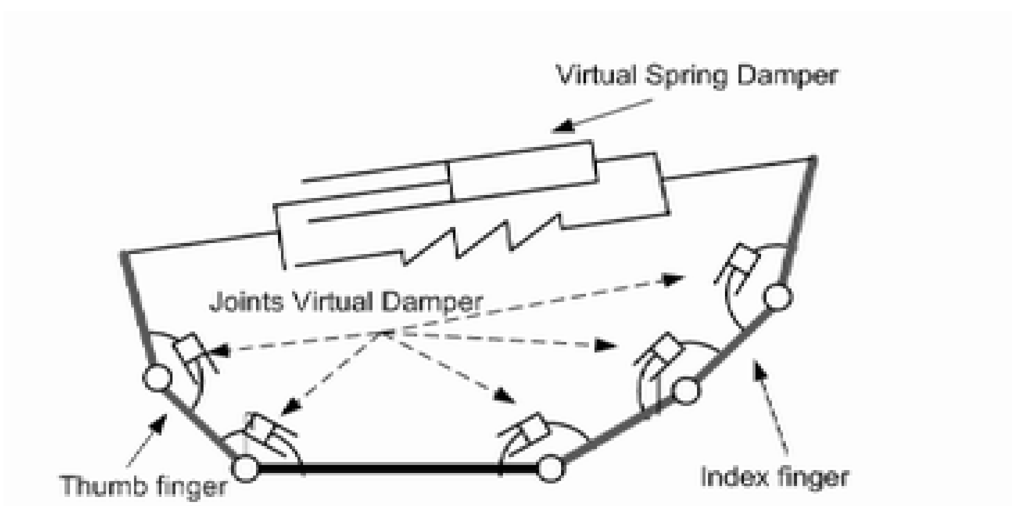

Fig. 3.2. Physical counterparts of the virtual forces

Higher values of k (virtual spring stiffness) result in faster movement of fingers as well as, higher grasping force. Thus by defining k proportional to EMG signal, amputee have control over speed of movement and grasping force.

The damping coefficient of finger joints, can change the final shape of fingers. The joints with lower damping tend to move more, while higher damped joints move more. The appropriate values of damping are evaluated based on trial and error to reach positions close to normal hand and they are held constant for further simulations.

3.3. Numerical Simulation

In order to show the effectiveness of the proposed control strategy, numerical simulations were conducted to grasp two different objects, based on the physical parameters of a hand system and objects summarized in Table 3.1.

The Adams software which is multi-body dynamic simulation software is used for numerical analysis. The software is capable to conduct information between Matlab/ Simulink software environment, hence the plant is modeled by Adams and controller is implemented in Matlab/Simulnk.

TABLE 3.1
PARAMETERS USED FOR SIMULATION

Parameter	Value
index finger link 1 length	5 cm
index finger link 2 length	2.5 cm
index finger link 3 length	2.5 cm
thumb finger link 1 length	4 cm
thumb finger link 2 length	3 cm
distance between thumb and index	6 cm
damping at joints	0.01 kg/s
virtual damping ratio	1
virtual spring stiffness	50 N/m
rectangular object width	2 cm
circular object radius	2 cm

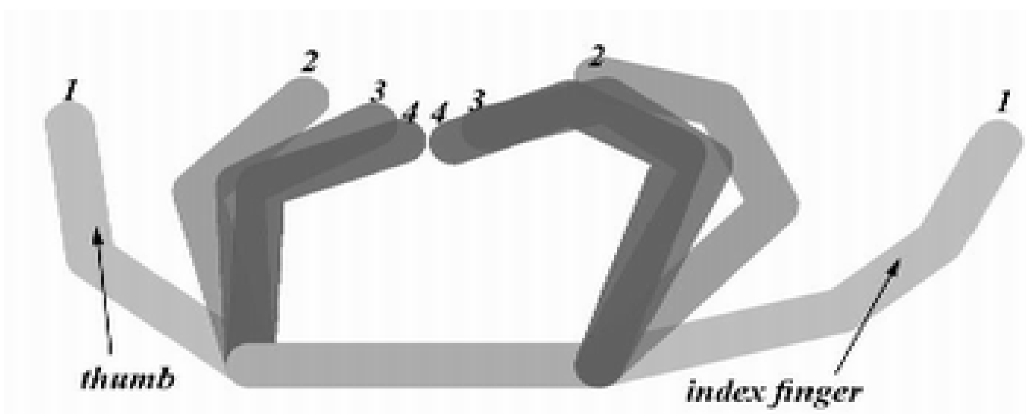

Fig. 3.3. Finger movements in 4 different position (0.25 sec. intervals)

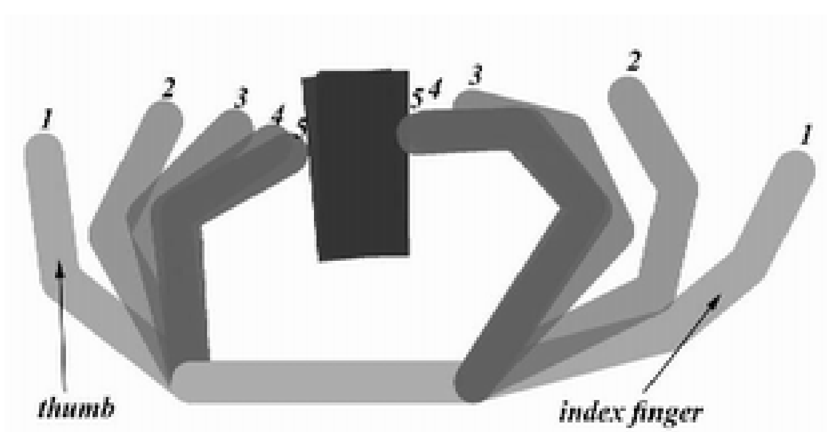

Fig. 3.4. Rectangular object grasping (0.25 sec intervals)

For first simulation, two fingers are modeled without any object in between. As shown in Fig.3.3, two fingers come together, and final position is close to normal hand coordination.

For the second simulation, a rectangular object is chosen to be grasped. The object is free to move in 2 dimensional plane, and contact and friction force are simulated between finger tip and the object. The object is placed at arbitrary final position of previous experiment. The finger movement at 0.25 sec time intervals and finger tip angles relative to palm are shown respectively in Figs. 3.4 and 3.5.

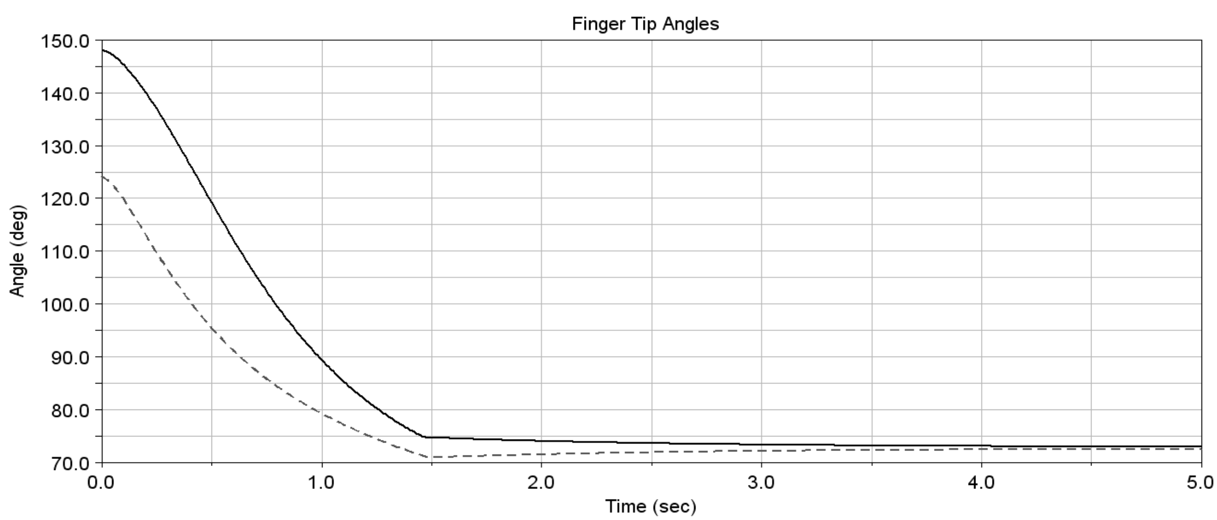

Fig. 3.5. Finger tips angle at rectangular object grasping
(index finger solid line and thumb finer dashed line)

As it is shown after contact with object at approximately 1.5 second the angles are not changing much. The small changes are due to object movements toward left.

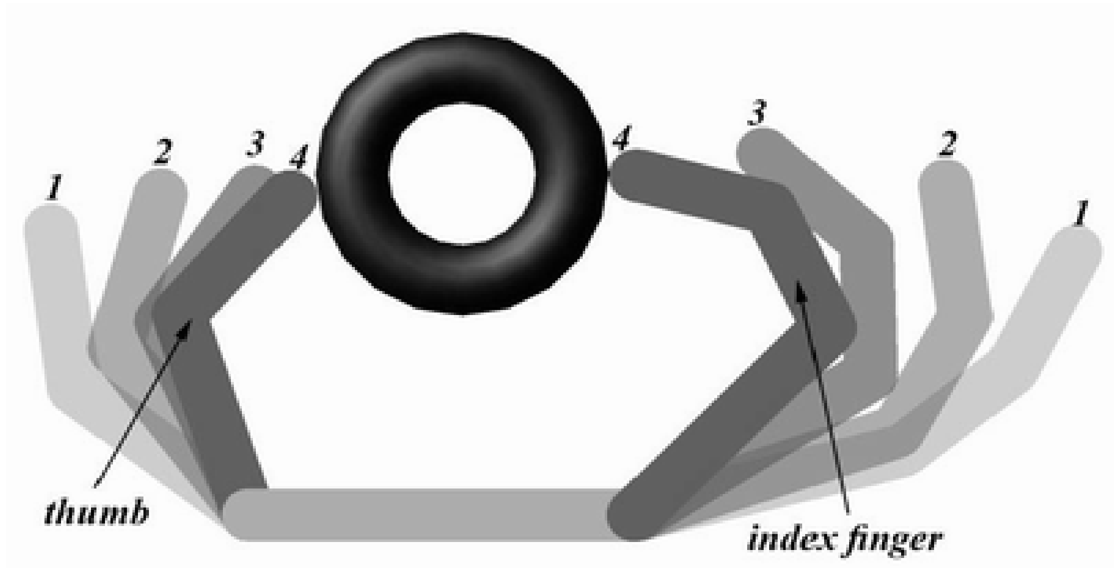

Fig. 3.6. Circular object grasping (0.25 sec intervals)

For third simulation a round object is selected. The object is not subjected to any constrain in 2 dimensional plane. The contact and friction force are defined between object and finger tip. The virtual spring coefficient which is proportional to EMG signal is assumed to be constant. Almost after 1 sec, the fingers contacted with the object. The finger movement at 0.25 sec time intervals and finger tip angles relative to palm are shown respectively in Fig.3.6 and Fig.3.7.

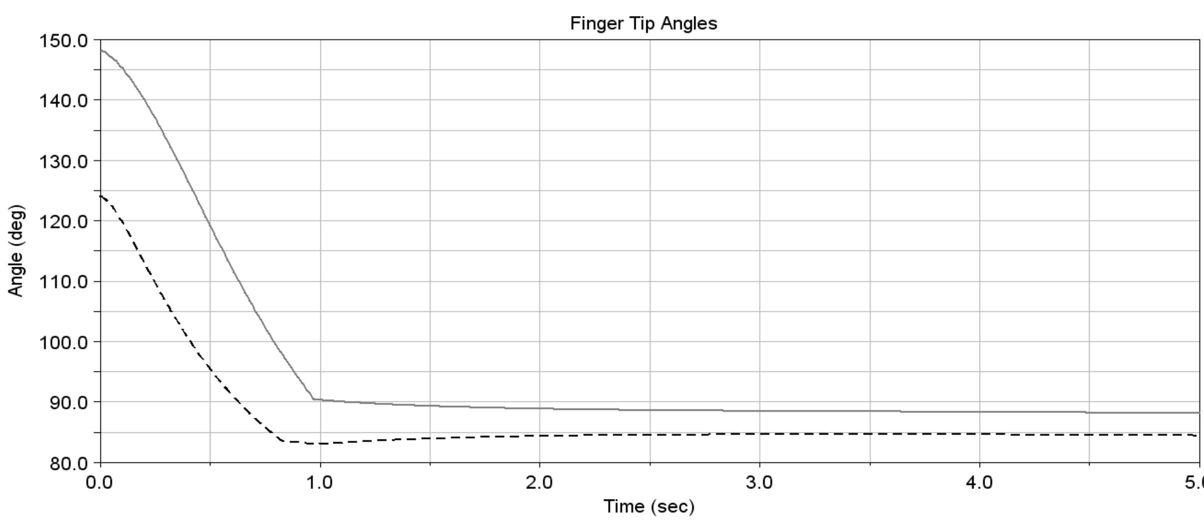

Fig. 3.7. Finger tips angle at circular object grasping
(index finger solid line and thumb finer dashed line)

Appropriate object position and friction force between fingers and object are important parameters that help successful grasping. For the case of a round object if the object has inappropriate position or friction is not enough, the grasping might be unstable, but guarantied successful grasping under all conditions require information about object shape and position which are not available for case of a prosthetic hand hence this control strategy is appropriate for most of the daily activities.

4. UNDERACTUATED PROSTHETIC HAND

4.1. Introduction

In underactuated mechanisms the number of actuators is less than their degree of freedom. These mechanisms are widely used in prosthetic hands because of two useful properties: the first advantage is less weight due to less actuator which is used in their design and the second advantage is easier control method.

Underactuation can be implemented through the use of passive elements like mechanical limits and springs leading to a mechanical adaptation of the finger to the shape of the object to be grasped. Underactuated robotic hands are the intermediate solution between fully actuated robotic hands for manipulation and simple grippers. It takes advantage of the mechanical intelligence embedded into the design of the hand allowing the shape adaptation of the fingers. In an underactuated finger, the actuation torque (or more generally wrench) is applied to the input of the finger and is transmitted to the phalanges through suitable mechanical design, e.g. linkages, pulleys and tendons, gears, etc.

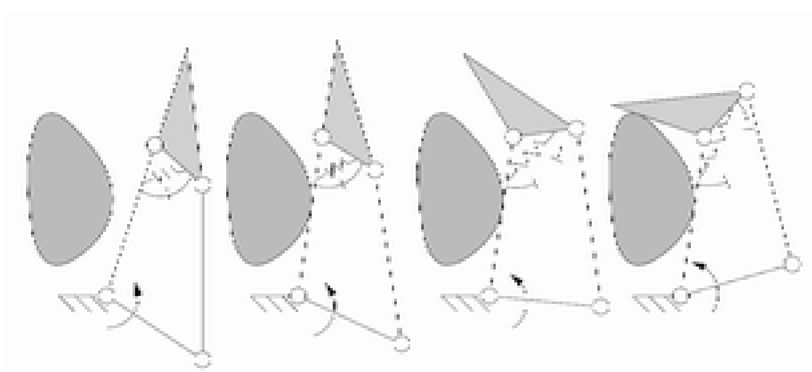

Fig 4.1.Closing sequence of a two-phalanx underactuated finger

An example of underactuated two-phalanx finger using linkages performing a typical closing sequence is illustrated in Fig. 4.1. The finger is actuated through the lower link, as shown by the arrow in the figure. Since there are two DOFs and one actuator, one (two minus one) elastic element is used. In the first two steps of the Figure, the finger behaves as a single rigid body in rotation about a fixed pivot. When the proximal phalanx makes contact with the object, the second phalanx is rotated away from the mechanical limit, and the finger is closing on the object since the proximal phalanx is constrained. During this phase, the actuator has to produce the force required to extend the spring. Finally, both phalanges are in contact with the object and the finger has completed the shape adaptation phase. The actuator force is distributed among the two phalanges in contact with the object. It should be noted that this sequence occurs with a continuous motion of the actuator. Notice also the mechanical limit that allows a pre-loading of the spring to prevent any undesirable motion of the second phalanx due to its own weight and/or inertial effects, and to prevent hyperextension of the finger. Springs are useful for keeping the finger from incoherent motion, but when the grasp sequence is complete, they still oppose the actuator force. Thus, they should be designed with the smallest stiffness possible, however sufficient to keep the finger from collapsing.

The basic property of the transmission system of an underactuated finger is to offer $n > 1$ DOF produced with fewer than n actuators. In Figure 2, the transmission stage consists of a five-bar linkage (the base joint is a double pivot) with two DOFs but one angle is initially constrained to a particular value with the spring and the mechanical limit.

4.2. Force analysis of underactuated finger

A two phalanx finger is considered in Fig.4.2. The input torque T_i is applied to the link a which transmits the torque to the whole finger trough phalanges. A rotational spring with force T is located at O which moves the phalanx back to its original position in absence of external force. The closing process is shown in Fig 4.2. Providing a mechanical limit can help in order to make pre-tension for the spring to prevent undesirable motion of the second phalanx and also hyper-flexion of the finger.

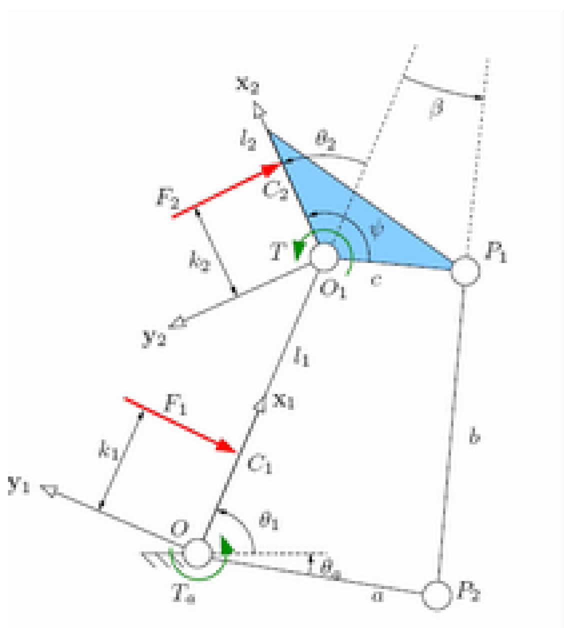

Fig.4.2. Underactuated hand model and exerted forces

To obtain the static model between inputs and outputs of the finger the virtual work principle is used. Equating the input and output virtual powers results

$$t^T \omega_i = f^T v \; t^T \omega_i = f^T v \tag{4-1}$$

Where t is the input torque vector exerted by the actuator and the spring, $\omega_i \, \omega_i$ is the rotational velocity vector, f is the vector of contact forces, and v is the velocity of the contact points along the normal vector of each phalanx. Contact forces are assumed to be normal to the phalanges and without friction. Each element in the above equation can be expressed as

$$t = \begin{bmatrix} T_i \\ T = -k\Delta\theta_2 \end{bmatrix} t = \begin{bmatrix} T_i \\ T = -k\Delta\theta_2 \end{bmatrix} \tag{4-2}$$

$$\omega_i = \begin{bmatrix} \dot{\theta}_i \\ \dot{\theta}_2 \end{bmatrix} \omega_i = \begin{bmatrix} \dot{\theta}_i \\ \dot{\theta}_2 \end{bmatrix} \tag{4-3}$$

$$f = \begin{bmatrix} f_1 \\ f_2 \end{bmatrix} f = \begin{bmatrix} f_1 \\ f_2 \end{bmatrix} \tag{4-4}$$

$$v = \begin{bmatrix} v_{C1}^T y1 \\ v_{C2}^T y2 \end{bmatrix} v = \begin{bmatrix} v_{C1}^T y1 \\ v_{C2}^T y2 \end{bmatrix} \tag{4-5}$$

The normal velocities of the contact point can be expressed as a Jacobian matrix $J_T \, J_T$ and the derivatives of the phalanx joint coordinates which is a natural choice, as $v = J_T \dot{\theta}$ $v = J_T \dot{\theta}$ or

$$\begin{bmatrix} v_{C1}^T y1 \\ v_{C2}^T y2 \end{bmatrix} = \begin{bmatrix} k_1 & 0 \\ k_2 + l_1 \cos\theta_1 & k_2 \end{bmatrix} \begin{bmatrix} \dot{\theta}_i \\ \dot{\theta}_2 \end{bmatrix} \begin{bmatrix} v_{C1}^T y1 \\ v_{C2}^T y2 \end{bmatrix} = \begin{bmatrix} k_1 & 0 \\ k_2 + l_1 \cos\theta_1 & k_2 \end{bmatrix} \begin{bmatrix} \dot{\theta}_i \\ \dot{\theta}_2 \end{bmatrix} \tag{4-6}$$

Through differential calculus, one also can relate vector $\omega_i \, \omega_i$ to the derivatives of the phalanges joint coordinates defined previously with an actuation Jacobian matrix J_A as $\dot{\theta} = J_A \omega_a \, \dot{\theta} = J_A \omega_a$ or

$$\begin{bmatrix}\dot{\theta}_i\\ \dot{\theta}_2\end{bmatrix}=\begin{bmatrix}X & Y\\ 0 & 1\end{bmatrix}\begin{bmatrix}\dot{\theta}_i\\ \dot{\theta}_2\end{bmatrix}$$ $$\begin{bmatrix}\dot{\theta}_i\\ \dot{\theta}_2\end{bmatrix}=\begin{bmatrix}X & Y\\ 0 & 1\end{bmatrix}\begin{bmatrix}\dot{\theta}_i\\ \dot{\theta}_2\end{bmatrix}$$

(4-7)

Where X=1 and

$$Y=\frac{c[l_1\sin(\theta_2-\psi)-a\sin(\theta_1-\theta_a+\theta_2-\psi)]}{a[l_1\sin(\theta_1-\theta_a)+c\sin(\theta_1-\theta_a+\theta_2-\psi)]}$$

$$Y=\frac{c[l_1\sin(\theta_2-\psi)-a\sin(\theta_1-\theta_a+\theta_2-\psi)]}{a[l_1\sin(\theta_1-\theta_a)+c\sin(\theta_1-\theta_a+\theta_2-\psi)]}$$

(4-8)

Finally, one obtains

$$f=J_T^{-T}J_A^{-T}t$$ $$f=J_T^{-T}J_A^{-T}t$$

(4-9)

which is the equation that provides a practical relationship between the actuator torque and contact forces. If the spring contribution is neglected the analytical expression are rather simple linear functions of the actuator torque,

$$f_1=\frac{(k_2-h\cos\theta_2)l_1}{a\,k_1k_2(\cot\beta\cos\alpha_1+\sin(\alpha_1))}T_a$$ $$f_1=\frac{(k_2-h\cos\theta_2)l_1}{a\,k_1k_2(\cot\beta\cos\alpha_1+\sin(\alpha_1))}T_a$$

(4-10)

$$f_2=\frac{h}{a\,k_2(\cot\beta\cos\alpha_1+\sin(\alpha_1))}T_a$$ $$f_2=\frac{h}{a\,k_2(\cot\beta\cos\alpha_1+\sin(\alpha_1))}T_a$$

(4-11)

where $\boldsymbol{h} = c(\cos(\theta_2 - \psi) - \sin(\theta_2 - \psi \cot[\![\beta)$ $\boldsymbol{h} = c(\cos(\theta_2 - \psi) - \sin(\theta_2 - \psi \cot[\![\beta)$ is the distance between point O_1 O_1 and the intersection of lines $(OO_1)(OO_1)$ and $(P_1P_2)(P_1P_2)$. Also, α_1 α_1 is the angle between link *a* and the first phalanx. It can be shown that

$$\cot\beta \cos\alpha_1 + \sin\alpha_1 = \frac{\sin X}{\sin\beta} \cot\beta \cos\alpha_1 + \sin\alpha_1 = \frac{\sin X}{\sin\beta}$$

(4-12)

where *X* is the angle between links *a* and *b.*

4.3. Design optimization

After obtaining the forces equation two consideration form the guidelines for design parameters selection: first grasp should be stable which means ejection should be prevented and differences between the phalanx forces should be minimum possible value. In Ejection phenomena the finger slide and push the object out instead of a secure grasping. To prevent ejection the exerted forces by each phalanx to the object should be positive. It is also desirable that forces at each phalanx to be close to their mean value and force distribute evenly between phalanxes which is referred to as force isotropy. So the conditions which should be satisfied can be expressed as:

$$\begin{cases} f_1 = f_2 \\ f_1 > 0 \quad and \quad f_2 > 0 \end{cases} \begin{cases} f_1 = f_2 \\ f_1 > 0 \quad and \quad f_2 > 0 \end{cases}$$

(4-13)

In order to have force isotropy it is necessary that forces by each phalanx are equal, but forces are function of contact position and θ_2 θ_2 angle hence it is a local property. Therefore if the object moves these conditions are not true anymore. However in this case, another step is necessary since h is a function of the design parameters and the angle $\theta_2\theta_2$. Furthermore, many design variables are available to satisfy the latter equation, namely a, b, c, and d.

For instance, if one chooses $a = b$, a known c (e.g. resulting from minimal distance considerations) and $\psi = \frac{\pi}{2}\psi = \frac{\pi}{2}$, a is completely defined as

$$a = \frac{2\, l_1 c \sin\theta_2 + c^2 + l_1^2}{2}\frac{\sqrt{A}}{B}$$ $$a = \frac{2\, l_1 c \sin\theta_2 + c^2 + l_1^2}{2}\frac{\sqrt{A}}{B}$$

(4-14)

with ,

$$A = (C-1)\big((C-1)c^2 + 2cCl_1 \sin(\theta_2) + C^2 l_1^2\big]$$

$$A = (C-1)\big((C-1)c^2 + 2cCl_1 \sin(\theta_2) + C^2 l_1^2\big]$$

(4-15)

$$B = -c^2 + Cc^2 - l_1 c \sin\theta_2 + 2Cl_1 c \sin\theta_2 + Cl_1^2$$

$$B = -c^2 + Cc^2 - l_1 c \sin\theta_2 + 2Cl_1 c \sin\theta_2 + Cl_1^2$$ (4-16)

$$C = -K\theta_2 + \frac{k_2}{k_2 + l_1 \cos\theta_2 + k_1}$$ $$C = -K\theta_2 + \frac{k_2}{k_2 + l_1 \cos\theta_2 + k_1}$$

(4-17)

The above mentioned relationship can be used in order achieving isotropic design. However, the isotropic property is not very robust with respect to design parameters, so it suggests using the following method.

If one obtains an isotropic and therefore stable design for a particular contact set $[(k]_{1}, k_{2}, \theta_{2})[(k]_{1}, k_{2}, \theta_{2})$, it may be of interest that the finger is also robust with respect to ejection around this isotropic point, in order to ensure that a deviation from this configuration does not lead to an unstable grasp. The final aim is to guaranty stability for all grasps if possible and satisfy certain "quality" based indices like the isotropy. An index that can be used to ensure the grasp stability, even if the proximal contact is lost, is:

$$\mu = \frac{\int_W \delta(k_2, \theta_2) dk_2 d\theta_2}{\int_W dk_2 d\theta_2} \mu = \frac{\int_W \delta(k_2, \theta_2) dk_2 d\theta_2}{\int_W dk_2 d\theta_2}$$

(4-18)

Where $\delta(k_2, \theta_2)$ $\delta(k_2, \theta_2)$ is a Kronecker-like symbol for characterizing the stability of the contact situation:

$$\delta(k_2, \theta_2) = \begin{cases} 1 \textit{ if the final grasp is stable} \\ 0 \textit{ otherwise} \end{cases} \delta(k_2, \theta_2) = \begin{cases} 1 \textit{ if the final grasp is stable} \\ 0 \textit{ otherwise} \end{cases}$$

(4-19)

This index is the ratio between the stable and unstable areas in the grasp-state plane of the finger. Contour plots of the index μ is illustrated in Fig.4.3. for a mechanically actuated finger. The optimal design parameter values can be obtained using the following plot. In our design equal lengths are considered for both phalanxes ($l_2/l_1=1$), so the optimal value for c/a is around 0.6.

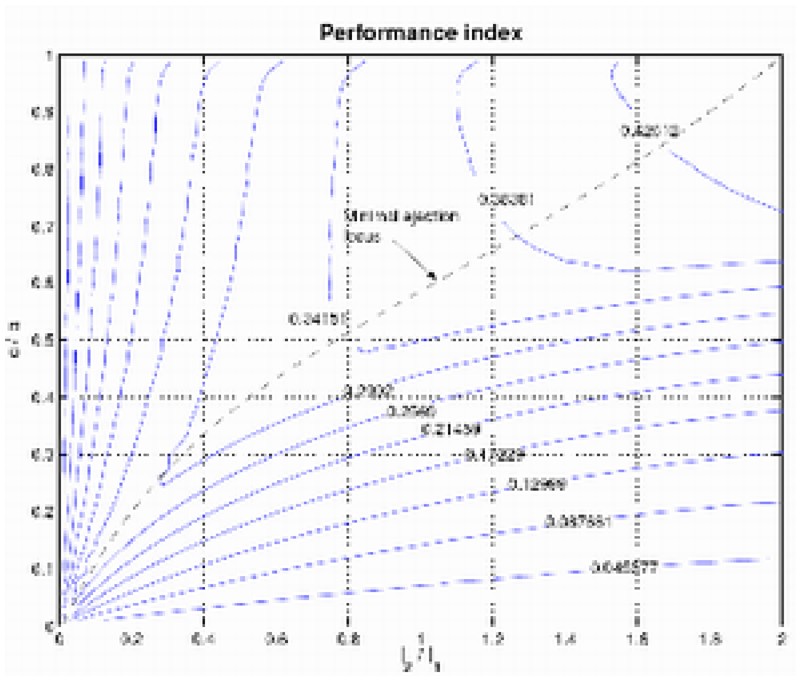

Fig 4.3. Performance index for linkage driven 2 phalanx underactuated hand

4.4. Control system

The control is aimed at exploiting the main properties of underactuation to perform motion tasks close to reference angles obtained by EMG signal. The ordinary task considered for design and development of the motion control law is the finger preshaping for the palmar grasp of a cylindrical object.

Kinematic coupling among the joints is related by the relation

$x_s = l_1\theta_1 + l_2(\theta_1 + \theta_2) x_s = l_1\theta_1 + l_2(\theta_1 + \theta_2)$

$$(4\text{-}20)$$

$\bar{x}_s = l_1\bar{\theta}_1 + l_2(\bar{\theta}_1 + \bar{\theta}_2)\bar{x}_s = l_1\bar{\theta}_1 + l_2(\bar{\theta}_1 + \bar{\theta}_2)$

$$(4\text{-}21)$$

The dynamic relation among the joints are derived in equations (10) and (11).

4.5. PD Control in the joint space with elastic compensation

Dynamic relation (20) and (21) is used to actively control the first joint and passively move the second joint. The proposed control law is a modified version of the standard PD control in the joint space with gravity compensation and is expressed as

$T_i = K_p\tilde{\theta} - K_D\dot{\theta} + g(\theta) + T_e\, T_i = K_p\tilde{\theta} - K_D\dot{\theta} + g(\theta) + T_e$

$$(4\text{-}22)$$

where $\tilde{\theta} = \theta_D - \theta$ $\tilde{\theta} = \theta_D - \theta$ is the joint position error defined as the difference between the reference set point θ_D θ_D and the current joint angle θ θ , $g(\theta)$ $g(\theta)$ is the estimation of joint gravitational torque, and K_p K_p and K_D K_D are the diagonal gain matrices for the proportional and derivative control actions, respectively. In addition to the standard PD control plus gravity compensation, an elastic term is introduced in order to compensate for the preload spring located between phalanxes joint.

The joint elastic torque is expressed as $T_e = k\Delta\theta_2\, T_e = k\Delta\theta_2$.

4.6. Numerical simulation

Based on results of optimal design a model of two phalanx finger is made in Adams software linked with Matlab/Simulink, which is shown in Fig. 4.3. Both phalanxes has the equal length and c/a ratio is 0.6 based on optimal design analysis. Torsion spring is located between two phalanxes. The revolute joint is located at joints and a motor is moving the finger which is shown by round arrow. A circular object is chosen to be grasped and the proposed controller is used to control finger movement.

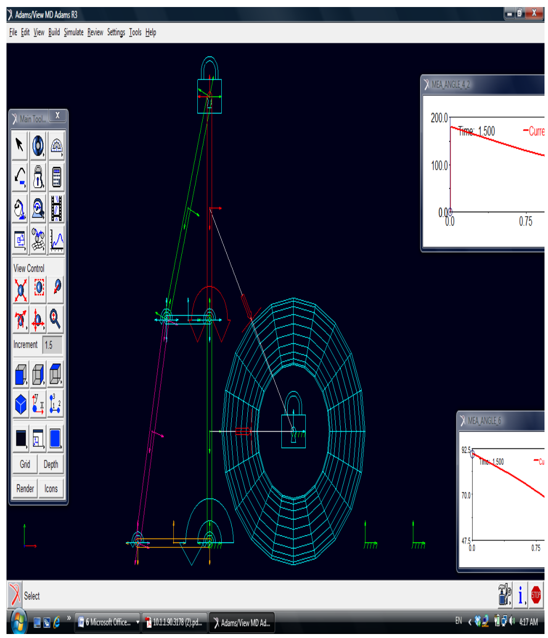

Fig.4.3. The two phalanx finger modeled in Adams software

By applying the control algorithm to the mechanism the finger can grasp the object. The grasping sequence is shown in Fig.4.4 .

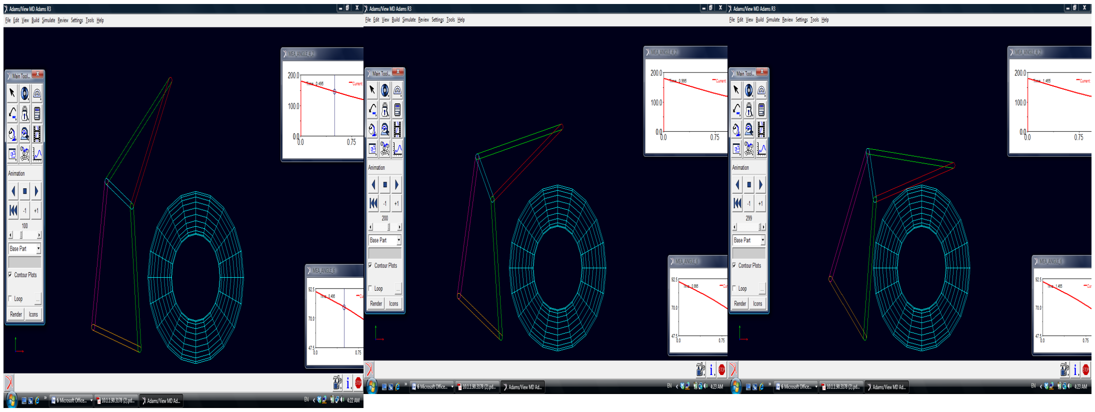

Fig. 4.4. The grasping sequence of a circular object by underactuated hand

The finger tip angle respect to horizontal plane is shown in Fig. 5. It starts from 90 degree and after first phalanx has contact with the object the rate of change of angle is changed.

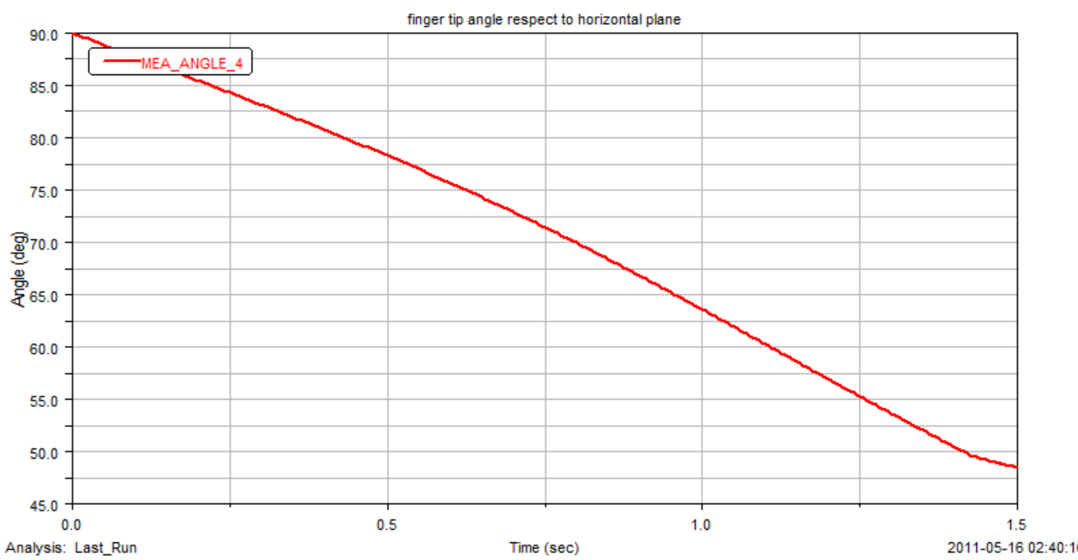

Fig. 4.5. Finger tip angle respect to horizontal plane for underactuated hand

Angle between two phalanxes is shown in Fig.4.6. The angle starts from 180 degree and gradually changes until second phalanx touches the object.

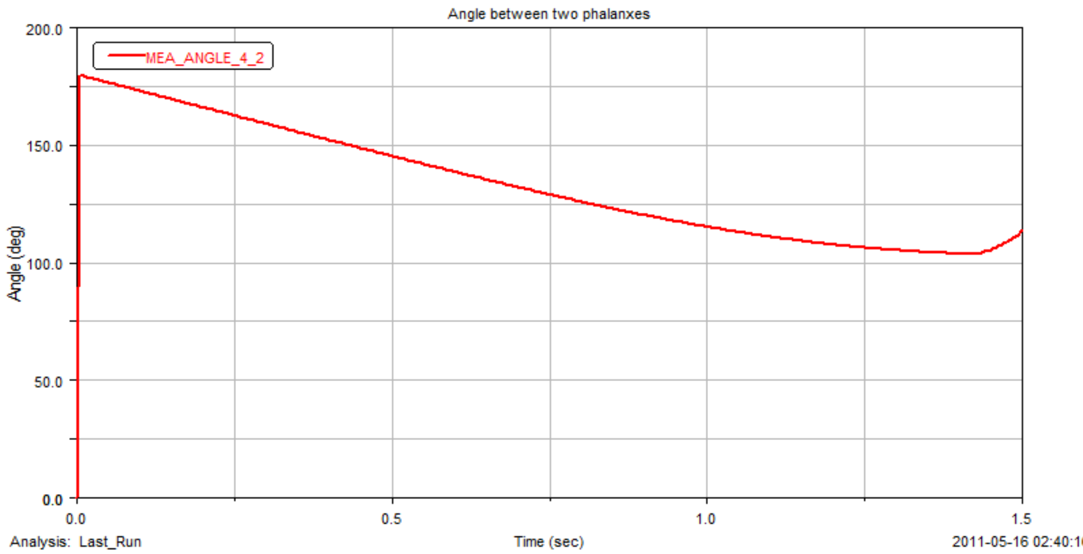

Fig.4.6. Angle between two phalanxes for underactuated hand

4.7. Comparison study between fully actuated and underactuated hand

Two general design which are fully actuated and underactuated and appropriate control methods for each of them are provided for prosthetic hand. In order to compare the functionality of these two methods a fully actuated finger with the same dimension and with a similar object to grasp is simulated. Power grasping algorithm which described before is used in order to control the movement. The sequence of movement is shown in Fig. 4.7. The finger tip angle respect to horizontal plane is shown in Fig. 4.8 and the angle between two joints is shown in Fig. 4.9.

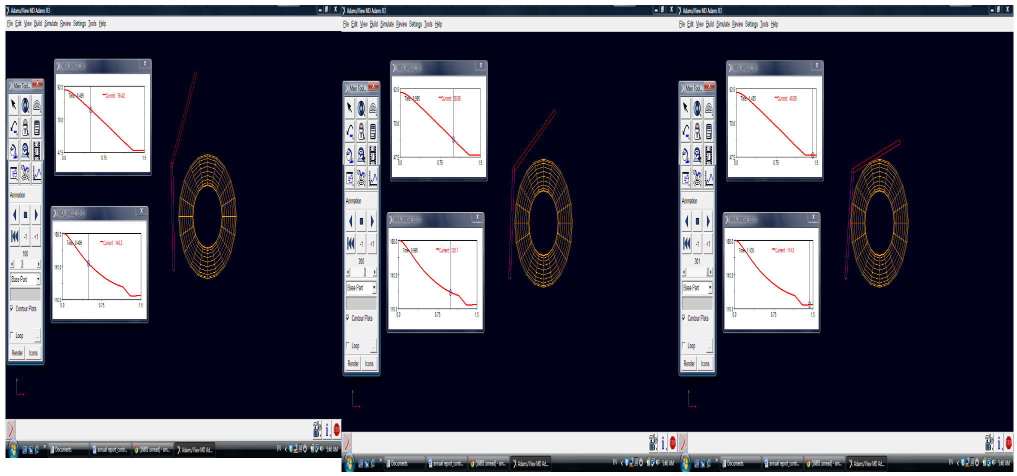

Fig. 4.7. The grasping sequence of a circular object by a fully actuated hand

As we can see both methods are capable to perform grasping and the graphs are very similar for both methods.

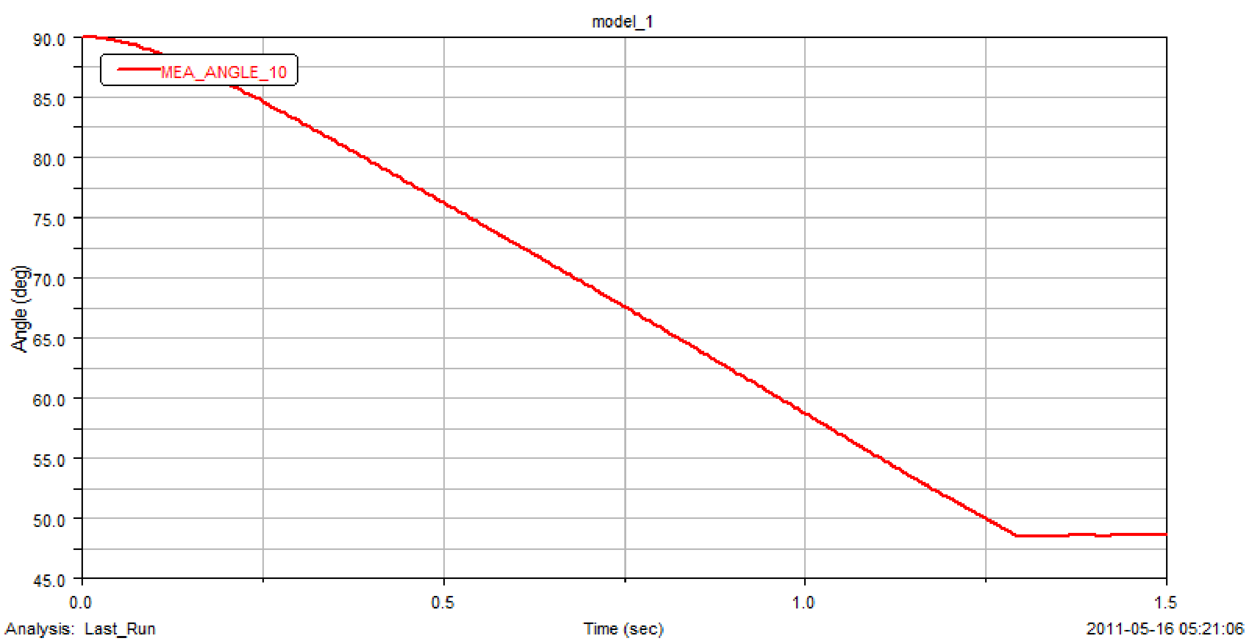

Fig.4.8. Finger tip angle respect to horizontal plane for fully actuated hand

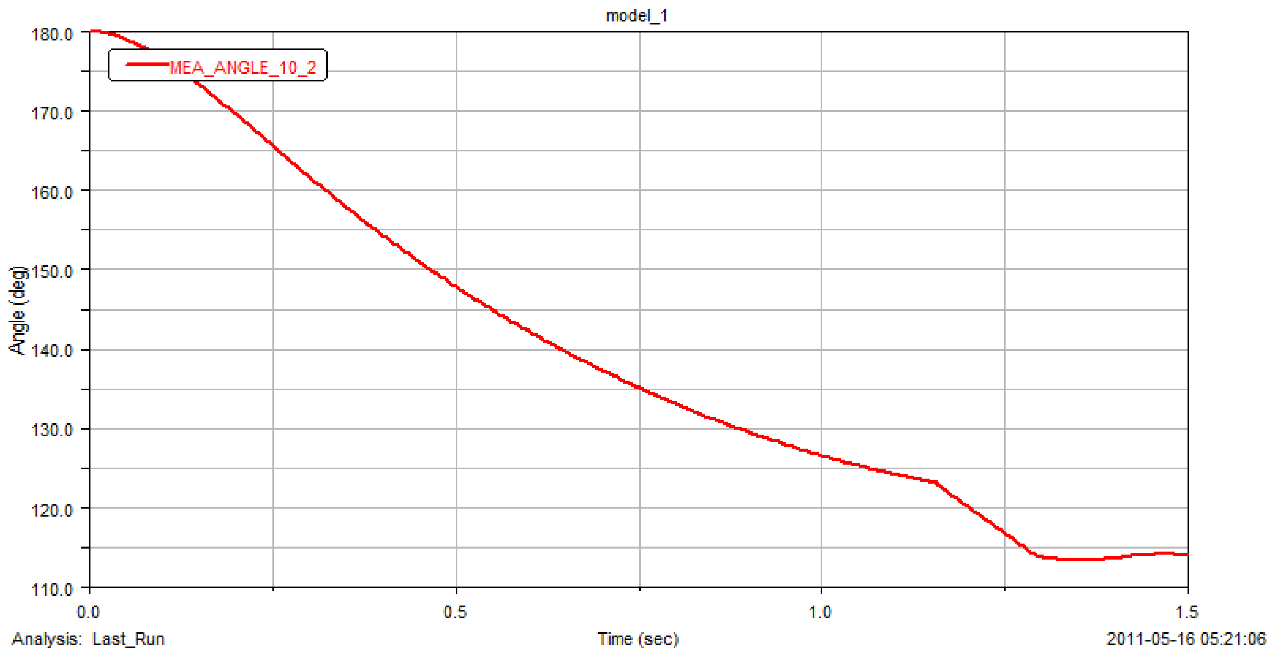

Fig.4.9. Angle between two phalanxes for fully actuated hand

5. ROBUST CONTROL OF A PROSTHETIC HAND

A finger can be considered as a 3 link robot, while in extracting the model for angle estimation, the PIP joint (the second) angle is considered, the third link angle normally has about 70% of the second joint angle and the first link angle is not considered in this research. As a result a two-link planar robot is considered as a plant to investigate the control approach performance.

A dynamic model can be derived from the general Lagrange equation method. The modeling of a two-link planar nonlinear robotic system with assumption of only masses in the two joints can be found in the literature, e.g., [3, 4]. However, in practice, the robot arms have their mass distributed along their arms, not only masses in the joints as assumed. Thus, it is desired to develop a detailed model for two-link planar robotic systems with the mass distributed along the arms. We present a new detailed consideration of any mass distributions along robot arms in addition to the joint mass. Moreover, it is also necessary to consider numerous uncertainties in parameters and modeling. Thus, robust control, robust adaptive control and learning control become important when knowledge of the system is limited. We need robust stabilization of uncertain robotic systems and furthermore robust performance of these uncertain robotic systems. Robust stabilization problem of uncertain robotic control systems has been discussed in [21-23, 24-26] and many others. Also, adaptive control methods have been discussed in [21,27] and many others. Because the closed-loop control system pole locations determine internal stability and dominate system performance, such as time responses for initial conditions, papers [26,28] consider a robust pole clustering in vertical strip on the left half splane to consider robust stability degree and degree of coupling effects of a slow subsystem (dominant model) and the other fast subsystem (non-dominant model) in a two-time-scale system. A control design method to place the system poles robustly within a vertical strip has been discussed in [26, 28-30], especially [26] for robotic systems. However, as mentioned above, for accurate prosthetic hand control there is a need of a detailed and practical two-link planar robotic system modeling with the practically distributed robotic arm mass for control.

Therefore a practical and detailed two-link planar robotic systems modeling and a robust control design for this kind of nonlinear robotic systems with uncertainties considered for robust control approach with both H∞ disturbance rejection and robust pole clustering in a vertical strip. The design approach is based on the new developing two-link planar robotic system models, nonlinear control compensation, a linear quadratic regulator theory and Lyapunov stability theory.

5.1. Modeling of Prosthetic Hand Systems

The dynamics of a rigid revolute robot manipulator can be described as the following nonlinear differential equation [21, 22, 26, 30]:

$$\mathbf{F_c} = \mathbf{M(q)\ddot{q} + V(q,\dot{q})\dot{q} + N(q,\dot{q})F_c} = \mathbf{M(q)\ddot{q} + V(q,\dot{q})\dot{q} + N(q,\dot{q})}$$

(5-1)

$$\mathbf{N(q,\dot{q}) = G(q) + F_d\dot{q}} + \square_s\mathbf{(\dot{q})N(q,\dot{q}) = G(q) + F_d\dot{q}} + \square_s\mathbf{(\dot{q})}$$

(5-2)

where $\mathbf{M(q)}\mathbf{M(q)}$ is an n x n inertial matrix, $\mathbf{V(q,\dot{q})}\mathbf{V(q,\dot{q})}$ an n x n matrix containing centrifugal and coriolis terms, $\mathbf{G(q)}\mathbf{G(q)}$ an n x 1 vector containing gravity terms, q(t) an n x1 joint variable vector, $\mathbf{F_c}\,\mathbf{F_c}$ an n x1 vector of control input functions (torques, generalized forces), $\mathbf{F_d}\,\mathbf{F_d}$ an n x n diagonal matrix of dynamic friction coefficients, and $\mathbf{F_s(\dot{q})}\,\mathbf{F_s(\dot{q})}$ an n x 1 Nixon static friction vector.

However, the dynamics of the robotic system (4,5) in detail is needed for designing the angle control, i.e., especially, what matrices $\mathbf{M(q)}\;\mathbf{M(q)}$, $\mathbf{V(q,\dot{q})}\mathbf{V(q,\dot{q})}$ and $\mathbf{G(q)}\mathbf{G(q)}$ are.

Consider a two-link planar robotic system representing the prosthetic hand finger in Fig. 5.1, where the system has its joint mass $\mathbf{m_1}\,\mathbf{m_1}$ and $\mathbf{m_2}\,\mathbf{m_2}$ of joints 1 and 2, respectively, robot arms mass $\mathbf{m_{1r}}\,\mathbf{m_{1r}}$ and $\mathbf{m_{2r}}\,\mathbf{m_{2r}}$ distributed along arms 1 and 2 with their lengths $\mathbf{l_1}\,\mathbf{l_1}$ and $\mathbf{l_2}\,\mathbf{l_2}$, generalized coordinates $\mathbf{q_1}\,\mathbf{q_1}$ and $\mathbf{q_2}\,\mathbf{q_2}$, i.e., their rotation angles, $\mathbf{q = [q_1, q_2]}\ \mathbf{q = [q_1, q_2]}$, control torques (generalized forces) $\mathbf{f_1}\,\mathbf{f_1}$ and $\mathbf{f_2}\,\mathbf{f_2}$, $\mathbf{F_c = [f_1, f_2]}\,\mathbf{F_c = [f_1, f_2]}$.

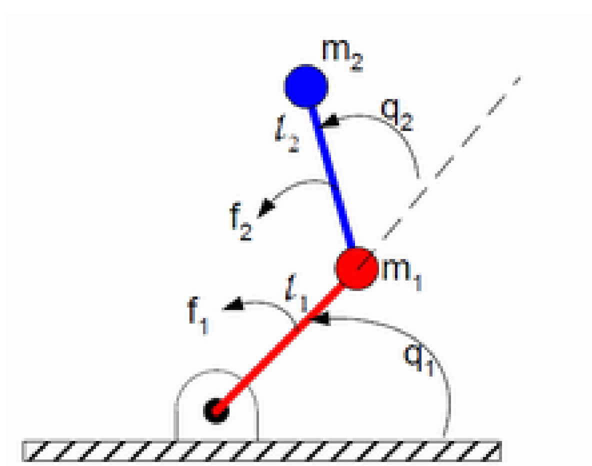

Fig 5.1- A two link robot system representing prosthetic hand

5.2. Robust Control

In view of possible uncertainties, the terms in (4,5) can be decomposed without loss of any generality into two parts, i.e., one is known parts and another is unknown perturbed parts as follows [22, 26]:

$$\mathbf{M} = \mathbf{M_0} + \Delta\mathbf{M}, \qquad \mathbf{N} = \mathbf{N_0} + \Delta\mathbf{N}, \qquad \mathbf{V} = \mathbf{V_0} + \Delta\mathbf{V}$$

$$\mathbf{M} = \mathbf{M_0} + \Delta\mathbf{M}, \qquad \mathbf{N} = \mathbf{N_0} + \Delta\mathbf{N}, \qquad \mathbf{V} = \mathbf{V_0} + \Delta\mathbf{V}$$

(5-3)

where $\mathbf{M_0}$ $\mathbf{M_0}$, $\mathbf{N_0}$ $\mathbf{N_0}$, $\mathbf{V_0}$ $\mathbf{V_0}$ are known parts, $\Delta\mathbf{M}$ $\Delta\mathbf{M}$, $\Delta\mathbf{N}$ $\Delta\mathbf{N}$, $\Delta\mathbf{V}$ $\Delta\mathbf{V}$ are unknown parts. Then, the models in previous chapter can be used not only for the total uncertain robotic systems with uncertain parameters, but also for a known part with their nominal parameters of the systems.

Following [26], we develop the torque control law as two parts as follows:

$$\mathbf{F_c} = \mathbf{M_0(q)\ddot{q}_d} + \mathbf{V_0(q,\dot{q})\dot{q}} + \mathbf{N_0(q,\dot{q})} - \mathbf{M_0(q)u}$$

$$\mathbf{F_c} = \mathbf{M_0(q)\ddot{q}_d} + \mathbf{V_0(q,\dot{q})\dot{q}} + \mathbf{N_0(q,\dot{q})} - \mathbf{M_0(q)u}$$

(5-4)

where the first part consists of the first three terms in the right side of (7), the second part is the term of u that is to be designed for the desired disturbance rejection and pole clustering, $\mathbf{q_d}$ $\mathbf{q_d}$ is the desired trajectory of q, however, the coefficient matrices are with all nominal parameters of the system. Define an error between the desired $\mathbf{q_d}$ $\mathbf{q_d}$ and the actual q as:

$$\mathbf{e} = \mathbf{q_d} - \mathbf{q}$$ $$\mathbf{e} = \mathbf{q_d} - \mathbf{q}$$

(5-5)

From (4) and (6)–(8), it yields:

$$\bar{\mathbf{e}} = \mathbf{M^{-1}(q)[\Delta M(q)\ddot{q}_d + \Delta V(q,\dot{q})\dot{q} + \Delta N(q,\dot{q}) + M_0(q)u] = w + E\dot{e} + Fu + u}$$
$$\bar{\mathbf{e}} = \mathbf{M^{-1}(q)[\Delta M(q)\ddot{q}_d + \Delta V(q,\dot{q})\dot{q} + \Delta N(q,\dot{q}) + M_0(q)u] = w + E\dot{e} + Fu + u}$$

(5-6)

$$\mathbf{E} = -\mathbf{M^{-1}(q)\Delta V(\square,\dot{q})}$$ $$\mathbf{E} = -\mathbf{M^{-1}(q)\Delta V(\square,\dot{q})},$$

$$\mathbf{F} = -\mathbf{M^{-1}(q)\Delta M(q)}, \qquad \mathbf{w} = -\mathbf{F\ddot{q}_d - E\dot{q}_d + M^{-1}\Delta N}$$
$$\mathbf{F} = -\mathbf{M^{-1}(q)\Delta M(q)}, \qquad \mathbf{w} = -\mathbf{F\ddot{q}_d - E\dot{q}_d + M^{-1}\Delta N}$$ (5-7)

From [26], we can have the fact that their norms are bounded:

$$\|\mathbf{w}\| < \delta_w, \qquad \|\mathbf{E}\| < \delta_e, \qquad \|\mathbf{F}\| < \delta_f$$ $$\|\mathbf{w}\| < \delta_w, \qquad \|\mathbf{E}\| < \delta_e, \qquad \|\mathbf{F}\| < \delta_f$$

(5-8)

Then, it leads to the state space equation as:

$$\dot{\mathbf{x}} = \mathbf{Ax + Bu + B[0\ E]\square + BFu + Bw}$$ $$\dot{\mathbf{x}} = \mathbf{Ax + Bu + B[0\ E]\square + BFu + Bw}$$

(5-9)

$$x = \begin{bmatrix} e \\ \dot{e} \end{bmatrix} = [e_1\ e_2\ \dot{e}_1\ \dot{e}_2]', \qquad A = \begin{bmatrix} 0 & I \\ 0 & \square \end{bmatrix}, \qquad B = \begin{bmatrix} 0 \\ I \end{bmatrix}$$

$$x = \begin{bmatrix} e \\ \dot{e} \end{bmatrix} = [e_1\ e_2\ \dot{e}_1\ \dot{e}_2]', \qquad A = \begin{bmatrix} 0 & I \\ 0 & \square \end{bmatrix}, \qquad B = \begin{bmatrix} 0 \\ I \end{bmatrix}$$

(5-10)

The last three terms denote the total uncertainties in the system. The desired trajectory q_d q_d for manipulators to follow is to be bounded functions of time. Its corresponding velocity $\dot{q}_{\square}$ $\dot{q}_{\square}$ and acceleration $\bar{q}_{\square}$ $\bar{q}_{\square}$, as well as itself q_d q_d , are assumed to be within the physical and kinematic limits of manipulators. They may be conveniently generated by a model of the type:

$$\bar{q_d}(t) + K_v \dot{q}_d(t) + K_p q_d(t) = r(t)$$

$$\bar{q_d}(t) + K_v \dot{q}_d(t) + K_p q_d(t) = r(t)$$

(5-11)

where $r(t)$ $r(t)$ is a 2-dimensional driving signal and the matrices K_v K_v and K_p K_p are stable.

The design objective is to develop a state feedback control law for control u in (7) as

$$u(t) = Kx(t)$$

$$u(t) = Kx(t)$$

(5-12)

such that the closed-loop system:

$\dot{\mathbf{x}} = (\mathbf{A} - \mathbf{BK} + \mathbf{B}[\mathbf{0}\ \mathbf{E}] - \square\mathbf{FK})\mathbf{x} + \mathbf{Bw}$ $\dot{\mathbf{x}} = (\mathbf{A} - \mathbf{BK} + \mathbf{B}[\mathbf{0}\ \mathbf{E}] - \square\mathbf{FK})\mathbf{x} + \mathbf{Bw}$

(5-13)

has its poles robustly lie within a vertical strip Ω:

$\lambda(\mathbf{A_c}) \in \boldsymbol{\Omega} = \{\mathbf{s} = \mathbf{x} + \mathbf{jy} | -\boldsymbol{\alpha_2} < x < -\boldsymbol{\alpha_1} \leq \mathbf{0}\}$
$\lambda(\mathbf{A_c}) \in \boldsymbol{\Omega} = \{\mathbf{s} = \mathbf{x} + \mathbf{jy} | -\boldsymbol{\alpha_2} < x < -\boldsymbol{\alpha_1} \leq \mathbf{0}\}$

(5-14)

and a δ-degree disturbance rejection from the disturbance ω to the state $\mathbf{x}$, i.e.,

$\|\mathbf{T_{xw}(s)}\|_\infty = \left\|(\mathbf{sI} - \mathbf{A_c})^{-1}\mathbf{B}\right\|_\infty \leq \boldsymbol{\delta}$ $\|\mathbf{T_{xw}(s)}\|_\infty = \left\|(\mathbf{sI} - \mathbf{A_c})^{-1}\mathbf{B}\right\|_\infty \leq \boldsymbol{\delta}$

(5-15)

$\mathbf{A_c} + \mathbf{A} - \mathbf{BK} + \mathbf{B}[\mathbf{0}\ \mathbf{E}]_{\mathbf{BFK}}$ $\mathbf{A_c} + \mathbf{A} - \mathbf{BK} + \mathbf{B}[\mathbf{0}\ \mathbf{E}]_{\mathbf{BFK}}$

(5-16)

we derive the following robust control law to achieve this objective is discussed in [20,26].

Consider prosthetic hand uncertain system (15) with (4)–(18) where the unstructured perturbations in (10) with the norm bounds in (11), the disturbance rejection index $\delta \geq \mathbf{0}$ $\delta \geq \mathbf{0}$ in (17), the vertical strip Ω in (16) and a matrix $\mathbf{Q} > \mathbf{0}$ $\mathbf{Q} > \mathbf{0}$.

With the selection of the adjustable scalars ε_1 ε_1 and ε_2 ε_2, i.e.,

$\frac{1-\delta_f}{\delta_e} > \varepsilon_1 > 0$ $\frac{1-\delta_f}{\delta_e} > \varepsilon_1 > 0$,

$(1-\delta_f-\varepsilon_1\delta_e)\delta > \varepsilon_2 > 0$ $(1-\delta_f-\varepsilon_1\delta_e)\delta > \varepsilon_2 > 0$

(5-17)

there always exists a matrix $P > 0$ $P > 0$ satisfying the following Riccati equation:

$$A'_{\alpha 1}P + PA_{\alpha 1} - \left(1-\delta_f-\varepsilon_1\delta_e-\frac{\varepsilon_2}{\delta}\right)PBB'P + \left(\frac{\delta_e}{\varepsilon_1}\right)I + \left(\frac{1}{\varepsilon_2\delta}\right)I + Q = 0$$

$$A'_{\alpha 1}P + PA_{\alpha 1} - \left(1-\delta_f-\varepsilon_1\delta_e-\frac{\varepsilon_2}{\delta}\right)PBB'P + \left(\frac{\delta_e}{\varepsilon_1}\right)I + \left(\frac{1}{\varepsilon_2\delta}\right)I + Q = 0$$

(5-18)

where

$A_{\alpha 1} = A + \alpha_1 I = \begin{bmatrix} \alpha_1 I_2 & I_2 \\ 0 & \alpha_1 I_2 \end{bmatrix}$ $A_{\alpha 1} = A + \alpha_1 I = \begin{bmatrix} \alpha_1 I_2 & I_2 \\ 0 & \alpha_1 I_2 \end{bmatrix}$

(5-19)

Then, a robust pole-clustering and disturbance rejection control law in (7) and (14) to satisfy (17) and (18) for all admissible perturbations E and F in (11) is as:

$u = -Kx = -rB'Px$ $u = -Kx = -rB'Px$

(5-20)

if the gain parameter r satisfies the following two conditions:

(i) $r \geq 0.5$ and (i) $r \geq 0.5$ and

(5-21)

(ii) $2\alpha_2 P + A'P + PA - \left(\frac{\delta_e}{\varepsilon_1}\right)I - [2r(1+\delta_f)+\varepsilon_1\delta_e]PBB'P > 0$

(ii) $\quad 2\alpha_2 P + A'P + PA - \left(\frac{\delta_e}{\varepsilon_1}\right)I - [2r(1+\delta_f) + \varepsilon_1\delta_e]PBB'P > 0$

(5-22)

Proof for the approach is provided in [26, 28].

It is also noticed that:

$$BB' = \begin{bmatrix} 0 & 0 \\ 0 & I_2 \end{bmatrix} BB' = \begin{bmatrix} 0 & 0 \\ 0 & I_2 \end{bmatrix}$$

(5-23)

It is evident that condition (i) is for the $\alpha_1 \alpha_1$ degree stability and δ degree disturbance rejection, and condition (ii) is for the $\alpha_2 \alpha_2$ degree decay, i.e., the left vertical bound of the robust pole-clustering.

There is always a solution for relative stability and disturbance rejection in this form. It is because the Riccati equation (20) guarantees a positive definite solution matrix P, and thus there exists a Lyapunov function to guarantee the robust stability of the closed loop uncertain robotic systems. The nonlinear compensation part in (7) has a similar function to a feedback linearization.

5.3. Numerical Simulation

Based on the proposed control approach, a two link robot is modeled considering uncertainties. Then the input signal from sEMG-Angle estimation model is used as reference signal to the plant and the performance is evaluated.

The system parameters are: link mass: $\mathbf{m_2 = m_2 = 0.05Kg}$ $\mathbf{m_2 = m_2 = 0.05Kg}$, lengths $\mathbf{l_1 = l_2 = 0.03m}$ $\mathbf{l_1 = l_2 = 0.03m}$, angular positions $\mathbf{q_1, q_2 (rad) q_1, q_2 (rad)}$, applied, torques $\mathbf{f_1, f_2 (Nm) f_1, f_2 (Nm)}$.

The initial states are set as $\mathbf{q_1(0) = q_2(0) = 0}$ $\mathbf{q_1(0) = q_2(0) = 0}$, and $\mathbf{\dot{q}_1(0) = \dot{q}_2(0) = 0}$ $\mathbf{\dot{q}_1(0) = \dot{q}_2(0) = 0}$. The parametric uncertainties are assumed to satisfy (11) with $\delta_f = 0.05$ $\delta_f = 0.05$, $\delta_e = 0.4$ $\delta_e = 0.4$, $\delta_n = 0.1$ $\delta_n = 0.1$. Select the adjustable parameters $\varepsilon_1 = 0.01$ $\varepsilon_1 = 0.01$, $\varepsilon_2 = 0.01$ $\varepsilon_2 = 0.01$ from (19), disturbance rejection index $\delta = 0.1$ $\delta = 0.1$, the relative stability index $\alpha_1 = 0.1$ $\alpha_1 = 0.1$, and the left bound of vertical strip $\alpha_2 = 2000$ $\alpha_2 = 2000$ since we want a fast response. We solved the Riccati equation (20)

to get the solution matrix P and the gain matrix as:

$$\mathbf{P} = \begin{bmatrix} \mathbf{12693 I_2} & \mathbf{1584 I_2} \\ \mathbf{1584 I_2} & \mathbf{1643 I_2} \end{bmatrix}$$

$$\mathbf{K = rB'P = [950 I_2 \; 985 I_2]}$$

Numerical simulation is done in Matlab software. For the plant the above mentioned parameters is used. Two sets of simulation are done. In the first simulation nominal plant is used and for the second simulation the perturbed model considering uncertainty is tested. The input signal for both simulations is measured angles from the above mentioned experiments from PIP joint. For the third joint the 70% of the measured angle of PIP joint used which is a good estimate of that signal.

The system response with nominal plant and perturbed plant to the input signal respectively are shown in Fig. 9 and Fig. 10. As it is shown the input and output signals are close and system is capable of following the command signal with sufficient accuracy. Obviously the system has a better performance in case of nominal plant compare to the perturbed model in which the uncertainties are applied.

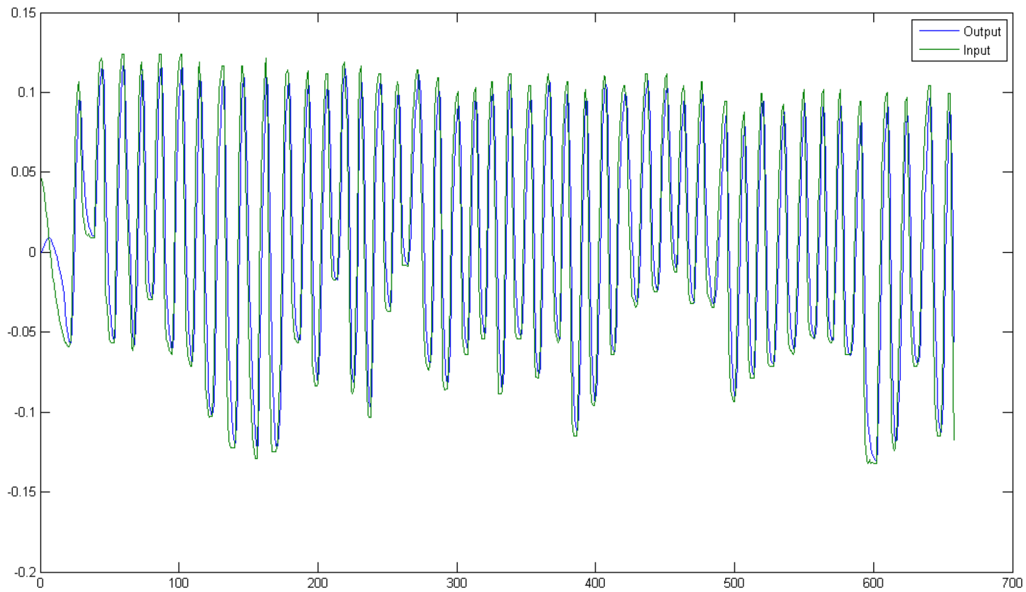

Fig. 5.2. System response to the nominal plant

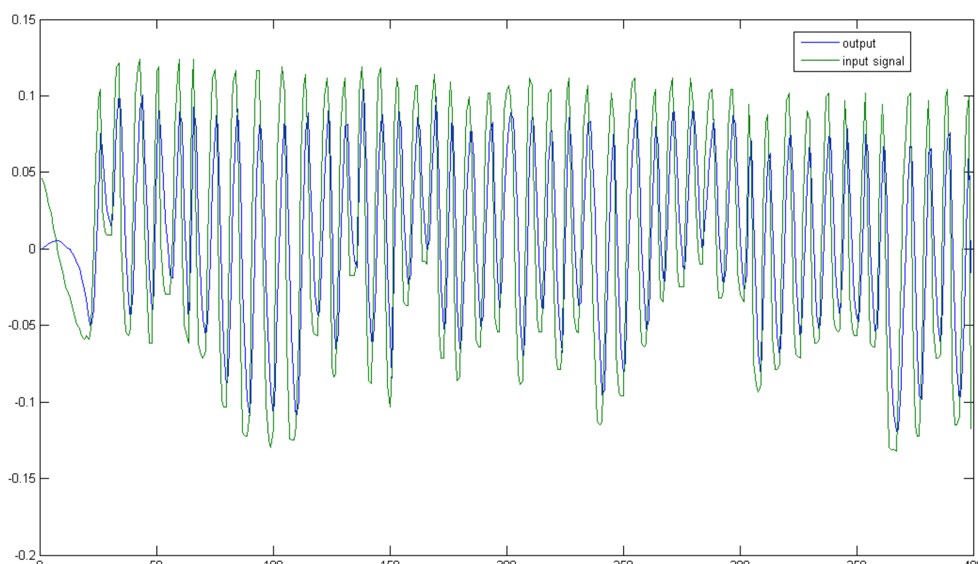

Fig.5.3 System response to the perturbed plant

6. EXPERIMENTAL TEST OF PROSTHETIC HAND CONTROL

6.1. Introduction

In the previous chapters several different ways for controlling the prosthetic hand have been investigated. In order to verify the results of these methods in practice some experiments are necessary. We have discussed two types of prosthetic hand in terms of mechanical design: fully-actuated hand and under-actuated hand, and as shown the control strategy related to each of these would be different. The fully actuated hands have more potential for different types of movements however control problem is more difficult. Under-actuated hands require less number of motors and their automatic adaptation property makes them more appropriate for control. These desirable properties made under-actuated hands more attractive for prosthetic hand designs. In our experiments we use an under-actuated hand as test setup.

6.2. System Input and Outputs

The objective of the embedded system design is that prosthetic hand fingers tracks a position signal as closely as possible. Here, the position is inferred from surface EMG (sEMG) signals obtained from the array of the sEMG sensors located at the arm. The sEMG data is processed by filtering and using a sensor fusion algorithm to facilitate the extraction of the best finger force estimates (Fig. 6.1).

According to this design the controller reference input is available by sEMG signal analysis. The feedback is angle of finger which is measured by angle sensors. For this purpose the angle flexible bending sensors are used. The sensor is a flexible strip which can measure bending through the change of the electrical resistance (Fig. 6.2). This sensor gives an overall measure of how much whole finger is moved.

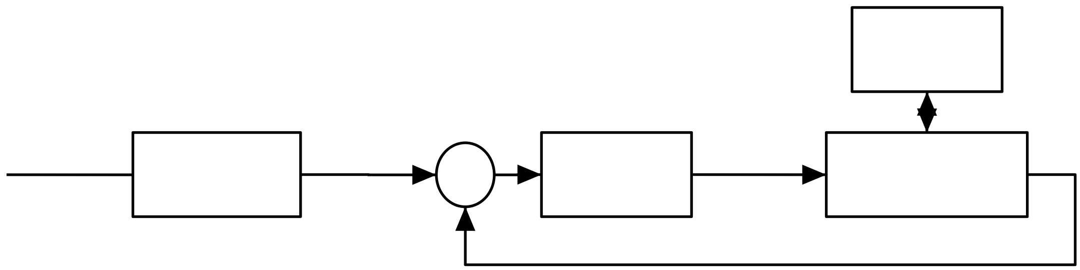

Fig. 6.1. Control Loop of Prosthetic Hand

Fig 6.2. Angle Sensor Used for Experiment

The output of the controller is command signal to the DC servo motors on the prosthetic hand which needs to be in form of PWM signal. The duty cycle of the signal controls motor position.

Although servo motor provide accurate position control, but motor angle is not equal to finger angle due to nonlinear dynamic of the prosthetic hand. Hence closed loop control is required to achieve desired angle of finger.

6.3. Plant Description

The prosthetic hand is equipped with 5 servo motors. Each of these motors is assigned to control movement of an individual finger (Fig. 6.3).

The hand is made of anodized aluminum to give enough strength and reduce the weight of prosthetic hand. It has 14 points of motion and 5 independent degrees of freedom provided by 5 electrical motors. The motors are DC servo motors and are controlled by PWM signal which is produced by microcontroller. The PWM signal should be between 1.5 and 2.5 ms. The 1.5 ms signal refers to fully closed position while 2.5 refers to fully open position.

There are some springs between motors and finger links. This makes the motors elastic and the springs are adjustable through some screws. The elastic actuators have the advantage of safe grip. This specification is necessary for a prosthetic hand and in case the hand exerts extra force elasticity in joints prevent damage.

Fig 6.3. Structure of Robotic Prosthetic Hand

6.4. Electrical Setup

The following modules of the PIC 32 are used for the implementation of the controller.

a. The Analog Input module
b. The Digital Output module
c. The Output Compare module
d. The UART module

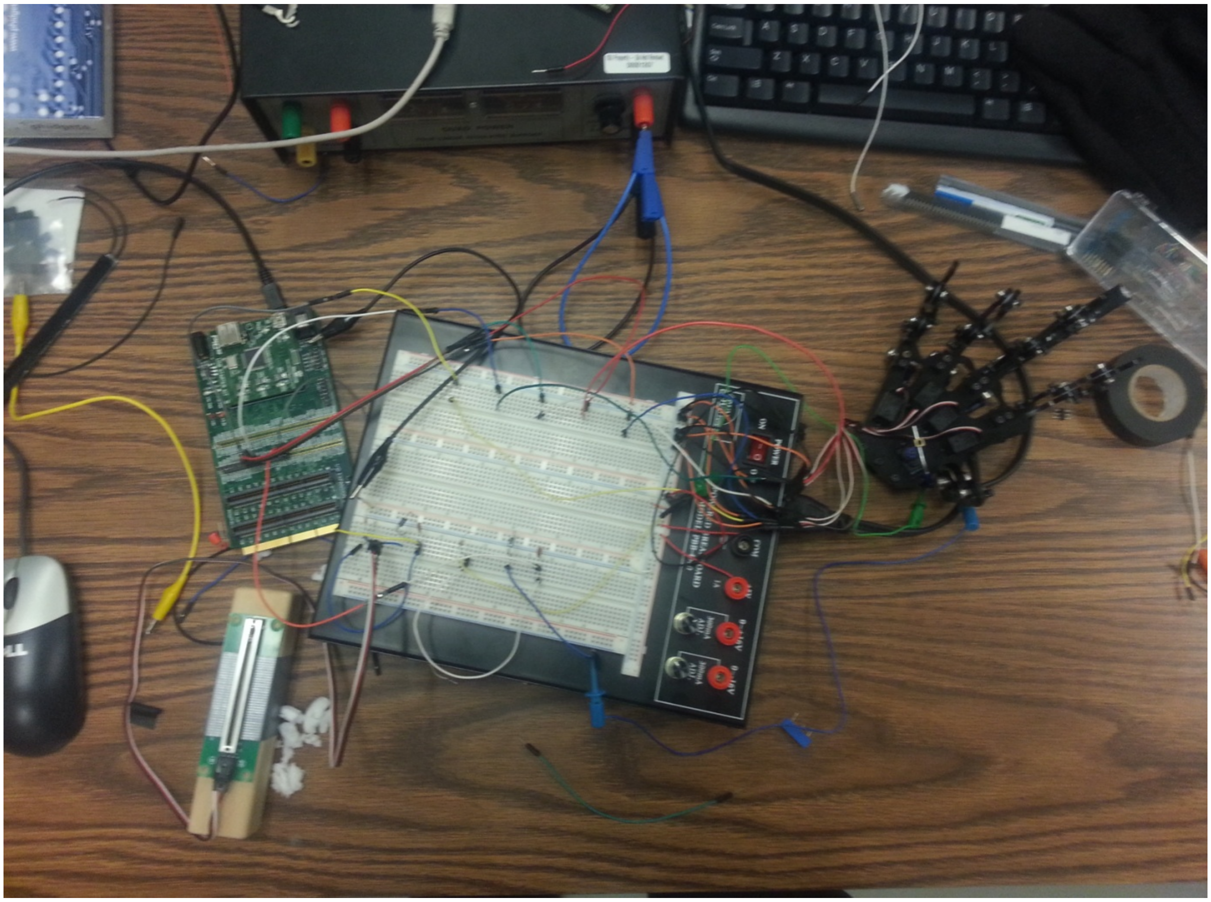

Fig. 6.4. Microcontroller and Electrical Circuit Used for Experiment

The Analog Input module is used for acquiring the sensory data from the bending angle sensors. The PIC 32 has an internal analog to digital converter (ADC) which has a 10-bit resolution so that it can distinguish up to 1024 different voltage values, usually in the range of 0 to 3.3 volts, and it yields 3mV resolution (Fig. 6.4). The Digital Output module of the PIC 32 is used to generate digital control signals based on the selected control strategy to the motor actuation stage. Depending on the error, a pulse width modulated (PWM) wave with a specific duty cycle is generated by the Output Compare module. The UART module in the PIC 32 is used to transmit the position data from the microcontroller to the PC via serial communication. In this design, a virtual com port was created to feed the data via USB cable to the computer. MATLAB® is used to read the signals from the ports. This enables the user to troubleshoot and see the performance and accuracy of the designed control strategy.

6.5. Motor Actuation Stage

The PWM wave from the Output Compare module is connected to the pin1 (1, 2EN). The PWM wave enables this H driver. The position of the motor depends on the duty cycle of the PWM wave from the Output Compare module which is a function of error.

Therefore the position of the motor is adjusted based on the error to achieve desired performance and accuracy.

This controls the finger to maintain the position based on the control strategy. Vcc1 and Vcc2 are connected to the 5V supply of the PIC 32 I/O board. This proposed design was tested on all fingers of a prosthetic hand prototype. Fig. 6.4 shows the test bed for the proposed design.

6.6. Control system

The control is aimed at exploiting the main properties of underactuation to perform motion tasks close to reference angles obtained by EMG signal. The ordinary task considered for design and development of the motion control law is the finger preshaping for the palmar grasp of a cylindrical object.

Kinematic coupling among the joints is related by the relation

$$x_s = l_1\theta_1 + l_2(\theta_1 + \theta_2) x_s = l_1\theta_1 + l_2(\theta_1 + \theta_2)$$

(6-1)

$$\bar{x}_s = l_1\bar{\theta}_1 + l_2(\bar{\theta}_1 + \bar{\theta}_2) \bar{x}_s = l_1\bar{\theta}_1 + l_2(\bar{\theta}_1 + \bar{\theta}_2)$$

(6-2)

The dynamic relation among the joints are derived in equations (6-1) and (6-2).

6.7. PD Control in the joint space with elastic compensation

Dynamic relation (1) and (2) is used to actively control the first joint and passively move the second joint. The proposed control law is a modified version of the standard PD control in the joint space with gravity compensation and is expressed as

$$T_i = K_p\tilde{\theta} - K_D\dot{\theta} + g(\theta) + T_e \, T_i = K_p\tilde{\theta} - K_D\dot{\theta} + g(\theta) + T_e$$

(6-3)

where $\tilde{\theta} = \theta_D - \theta$ $\tilde{\theta} = \theta_D - \theta$ is the joint position error defined as the difference between the reference set point θ_D θ_D and the current joint angle θ θ , $g(\theta)$ $g(\theta)$ is the estimation of joint gravitational torque, and K_p K_p and K_D K_D are the diagonal gain matrices for the proportional and derivative control actions, respectively. In addition to the standard PD control plus gravity compensation, an elastic term is introduced in order to compensate for the preload spring located between phalanxes joint.

The joint elastic torque is expressed as $T_e = k\Delta\theta_2$ $T_e = k\Delta\theta_2$.

6.8. Test Results

Data is acquired from the microcontroller through UART channel2 of the PIC 32 micro controller by a virtual Com port via USB at 57600 baud rate. The data from the microcontroller is converted into unit16 data type before it is transmitted through the UART. The PIC 32 microcontroller is running at 80 million instructions per second (MIPS) with its phase lock loop (PLL) activated. It is running at an external clock frequency of 8MHz with internal scaling enabled. Fig. 6.5 and Fig 6.6 depict the experimental results of the proposed design. The first experiment shows the step response of prosthetic hand, and the second one shows sine wave response.

The actual angle output from the Flexible Sensor closely follows the Commanded Position.

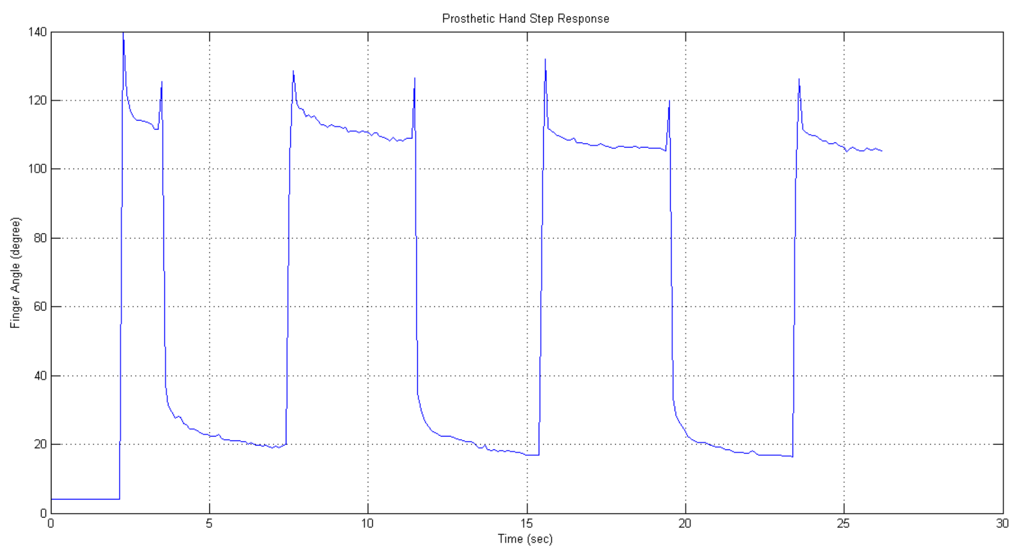

Fig 6.5. Step Response of Prosthetic Hand Finger

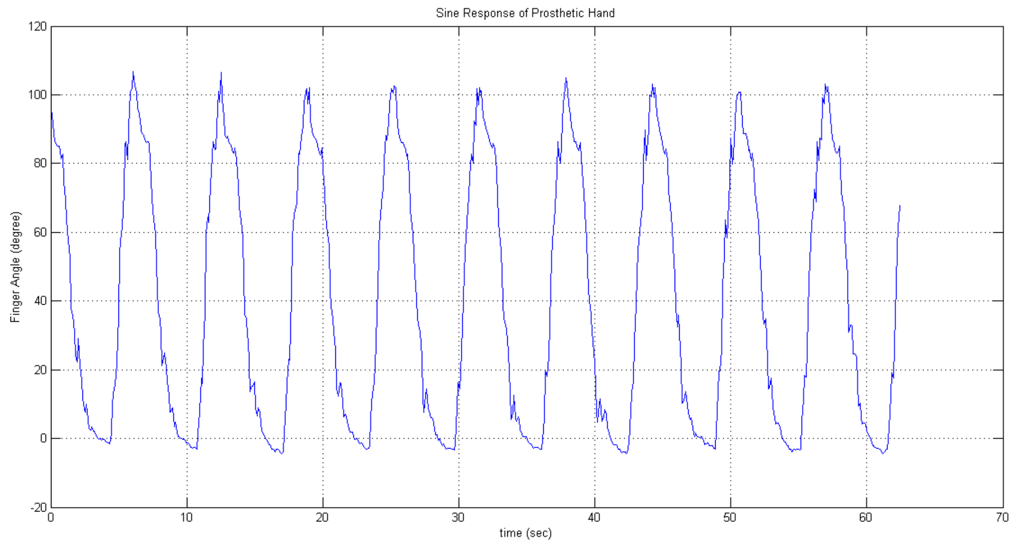

Fig 6.6. Sine Wave Response of Prosthetic Hand Finger

Based on simulation results in chapter 4 we expect similar finger movement. Fig. 6.7 and Fig.6.8 show the simulation result for step response and sine response respectively. There is a close similarity between simulation results and experimental results. The measurement noise and nonlinearity cause small difference between these two set of results.

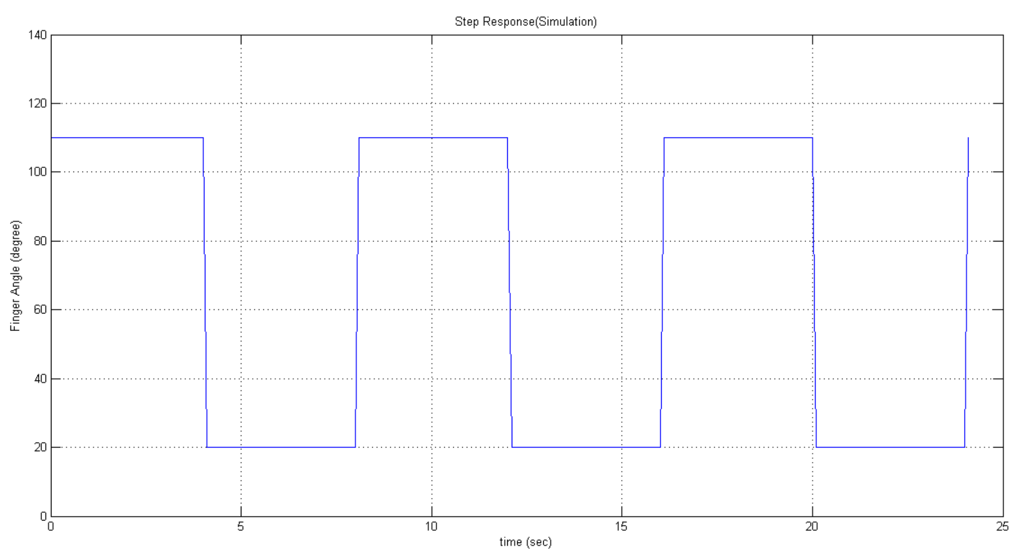

Fig 6.7. Step Response of Simulated Prosthetic Hand Finger

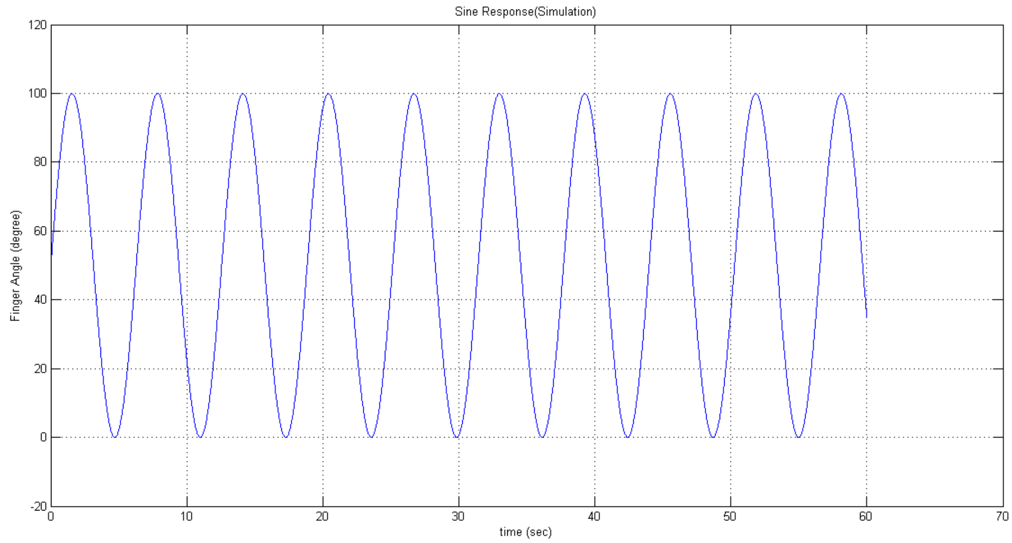

Fig 6.7. Sine Response of Simulated Prosthetic Hand Finger

7. CONCLUSION AND FUTURE WORKS

In this dissertation, power grasping control for fully actuated hand based on virtual spring damper hypothesis is investigated. This method is applicable in real time and does not rely on information about object shape to be grasped. Besides it can follow command line from EMG model.

Using the virtual spring damper precision grasping of fully actuated hand is covered in chapter 3. Similarly the method is applicable for real-time implementation and independent of information about object shape.

Section 4 discussed the underactuated hand design and optimization. Furthermore, position and force control method are presented and the results are compared with power grasping technique of fully actuated hand.

Section 5 covered robust control method to follow accurately angle command signal from EMG signal analysis in presence of plant uncertainty. In this part the EMG model is mixed with control technique and overall performance of the hand is analyzed.

Section 6 Covered the experimental test of proposed controller on a robotic prosthetic hand and evaluate its functionality.

Future works will be focused on other control strategies to follow command signal from EMG for both force and position models and mixing EMG model and control strategies. The fuzzy control is a powerful technique which will be studied to this aim. Sliding mode control is another option which is robust and also appropriate for nonlinear plants. This technique can be used for both force and position control of the prosthetic hand. Any other control technique which fits to this problem might be considered too.

Moreover, the precision grasping and power grasping techniques based on virtual spring damper, requires improvement to follow more precisely command signal from EMG signal. Current method is based on impedance control and it should be relate to force and position reference signal more accurately.

For underactuated hand, simple PID controller were studied which can be improved by more powerful control techniques like fuzzy control, neural networks, nonlinear control and any other applicable technique.

In this research we have published the following papers:

- Amir Fassih, D.Subbaram Naidu, Steve Chiu, Parmod Kumar, “Robust Control of a Prosthetic Hand Based on a Hybrid Adaptive Finger Angle Estimation”, WSEAS Conf. Athen, Greece, March 7-9,2012
- Amir Fassih, D.Subbaram Naidu, Steve Chiu, Parmod Kumar, “Design and Control of an Underactuated Prosthetic Hand”, Wseas Conf. Athen, Greece, March 7-9,2012
- Fassih, D.S. Naidu, S. Chiu, And M.P. Schoen, “Power Grasping of a Prosthetic Hand Based Upon Virtual Spring-Damper Hypothesis”, IASTED Int. Conf. Robotics And Applications, Cambridge, MA, November 1 – 3, 2010
- Fassih, D.S. Naidu, S. Chiu, And M.P. Schoen, “Precision Grasping of a Prosthetic Hand Based on Virtual Spring Damper Hypothesis”, Ieee 5th Cairo International Biomedical Engineering Conference, Cairo, Egypt, Dec 2010
- P. Kumar, C. H. Chen, A. Sebastian, M. Anugolu, C. Potluri, A. Fassih, Y. Yihun, A. Jensen, Y. Tang, S. Chiu, K. Bosworth, “An Adaptive Hybrid Data Fusion Based Identification of Skeletal Muscle Force With Anfis And Smoothing Spline

Curve Fitting”, International Conference On Fuzzy Systems, Taipei, Taiwan, June 27 - June 30, 2011.

References

[1] Amir Fassih, D.Subbaram Naidu, Steve Chiu, Parmod Kumar, “Robust Control of a Prosthetic Hand Based on a Hybrid Adaptive Finger Angle Estimation”, WSEAS Conf. Athen, Greece, March 7-9,2012

[2] Amir Fassih, D.Subbaram Naidu, Steve Chiu, Parmod Kumar, “Design and Control of an Underactuated Prosthetic Hand”, Wseas Conf. Athen, Greece, March 7-9,2012

[3] Fassih, D.S. Naidu, S. Chiu, And M.P. Schoen, “Power Grasping of a Prosthetic Hand Based Upon Virtual Spring-Damper Hypothesis”, IASTED Int. Conf. Robotics And Applications, Cambridge, MA, November 1 – 3, 2010

[4] Fassih, D.S. Naidu, S. Chiu, And M.P. Schoen, “Precision Grasping of a Prosthetic Hand Based on Virtual Spring Damper Hypothesis”, Ieee 5th Cairo International Biomedical Engineering Conference, Cairo, Egypt, Dec 2010

[5] P. Kumar, C. H. Chen, A. Sebastian, M. Anugolu, C. Potluri, A. Fassih, Y. Yihun, A. Jensen, Y. Tang, S. Chiu, K. Bosworth, “An Adaptive Hybrid Data Fusion Based Identification of Skeletal Muscle Force With Anfis And Smoothing Spline Curve Fitting”, International Conference On Fuzzy Systems, Taipei, Taiwan, June 27 - June 30, 2011.

[6] Mohammad Asghar Oskooei, Housheng Hu, “Myoelectric control systems, a survey”, *Biomedical Signal Processing and Control*, vol. 2, 2007, pp 275-294.

[7] Chiristian Cipriani, Franco Zaccone, Silvestro Micera, Chiara Carrozza, “On the shared control of an emg-controlled prosthetic hand: analysis of user-prosthesis interaction”, *IEEE Transaction on Robotics,* vol.24, No1, February 2008.

[8] Erik D Engeberg, Sanford G. Meek, “Backsptepping and sliding mode control hybridized for a prosthetic hand”, *IEEE Trans. on Neural Systems and Rehabilitation Engineering*, vol. 17, No.1, February 2009.

[9] D.E.Whitney, “Resolved motion rate control of manipulators and human prostheses”, *IEEE Trans. Man-Machine Syst.*, vol. MMS-10, No.2, 1969, pp.47– 53.

[10] Y. Nakamura, “Advanced robotics: redundancy and optimization”, Addison-Wesley, Reading, MA, 1991.

[11] N. Dechev, W.L. Cleghron, S. Naumann, Multiplefinger, “Passive adaptive grasp prosthetic hand”, *Mechanism and Machine Theory,* vol.36, 2001, pp.1157-1173.

[12] Ramiero Cabas, Luis Maria Cabas, Carlos Balaguer, “Optimized design of the underactuated robotic hand”, *Proceeding of the 2006 IEEE International Conferences on Robotics and Automation*, Orlando, Florida, May 2006.

[13] Da-Peng Yang, Jing-dong Zhao, Yi-kun Gu, Xin-qing Wang, Nan Li, Li Jiang, Hong Liu, Hai Huang, Da-wei Zhao, “An anthropomorphic robot hand develeoped based on underactuated mechanism and controlled by EMG signals”, *Journal of Bionic Engineering,* vol. 6, 2009, pp 255-263.

[14] Suguru Arimoto, Masahiro Sekimoto, “Human-like movements of robotic arms with redundant dofs: virtual spring-damper hypothesis to tackle the brenestein problem”, *Prec. of IEEE Int. Conf. on Robotics and Automation,* Orlando, Florida, May 2006.

[15] Jerry Pratt, Chee-Meng Chew, Ann Torres, Peter Dilworth, Gill Pratt, “Virtual model control: an intuitive approach for bipedal locomotion”, *The International Journal of Robotics Research,* vol. 20, No. 2, pp. 129-143, February 2001.

[16] Thomas Wimboeck, Christian Ott, Gerhard Hirzinger, "Passivity-based object-level impedance control for a multifingered hand" *Proceedings of the 2006 IEEE/RSJ, International Conference on Intelligent Robots and Systems,* Beijing, China,2006.

[17] Lionel Brignel,Thiery Laliberte, Clement Gosselin, "Underactuated robotic hand",Springer 2008.

[18] H. Kawasaki, T. Komatsu, and K. Uchiyama, "Dexterous anthropomorphic robot hand with distributed tactile sensor: Gifu hand II," *IEEE-ASME Transactions on Mechatronics,* vol. 7, no. 3, pp. 296-303, Sept. 2002.

[19] S. M. M. Zecca, M. C. Carrozza, & P. Dario, "Control of Multifunctional Prosthetic Hands by Processing the Electromyographic Signal," *Critical Reviews™ in Biomedical Engineering,* vol. 30, no. 4–6, pp. 459–485, 2002.

[20] C. Castellini, and P. van der Smagt, "Surface EMG in advanced hand prosthetics," *Biological Cybernetics,* vol. 100, no. 1, pp. 35-47, Jan. 2009.

[21] *O. Diane J. Atkins*, *M. Denise C.Y. Heard*, and *M. William H. Donovan*, "Epidemiologic overview of individuals with upper-limb loss and their reported research priorities," *Journal of Prosthetics and Orthotics* vol. 8, no. 1, pp. 2-11, 1996.

[22] D. H. Silcox, M. D. Rooks, R. R. Vogel *et al.*, "Myoelectric Prostheses - A Long-Term Follow-Up and A Study of The Use of Alternate Prostheses," *Journal of Bone and Joint Surgery-American Volume,* vol. 75A, no. 12, pp. 1781-1789, Dec. 1993.

[23] C. J. De Luca, “The use of surface electromyography in biomechanics,” *Journal of Applied Biomechanics,* vol. 13, no. 2, pp. 135-163, May 1997.

[24] M. B. I. Reaz, M. S. Hussain, and F. Mohd-Yasin, “Techniques of EMG signal analysis: detection, processing, classification and applications,” *Biological Procedures Online*, pp. 11-35, Mar. 14, 2006.

[25] R. M. a. P. A. Parker, *Electromyography: physiology, engineering, and noninvasive applications*, Hoboken, New Jersey, USA: John Wiley and Sons Inc., 2004.

[26] M. G. Amin, *Time-frequency spectrum analysis and estimation for nonstationary random processes*, p.^pp. 208-232, Melbourne, Australia: Longman Cheshire (AUS), 1992.

[27] A. M. S. a. D. L. Jones, “Optimal Kernels for Nonstationary Spectral Estimation,” *IEEE Transactions on Signal Processing,* vol. 43, no. 2, pp. 478-491, 1995.

[28] D. a. C. Graupe, William K., “Functional Separation of EMG Signals via ARMA Identification Methods for Prosthesis Control Purposes,” *IEEE Transactions on Systems, Man and Cybernetics,* vol. SMC-5, no. 2, pp. 252 - 259, 1975.

[29] M. H. Sherif, “A stochastic model of myoelectric signals for movement pattern recognition in upper limb prostheses,” University of California, Los Angeles, 1980, 1980.

[30] C. Yitong Zhou, R., and Bekey, G., “Estimation of intramuscular EMG signals from surface EMG signal analysis,” in IEEE International Conference on ICASSP'86: Acoustics, Speech, and Signal Processing, Tokyo, Japan 1986, pp. 1805 - 1808

[31] Z. W. Hefftner G, and Jaros GG., “The electromyogram (EMG) as a control signal for functional neuromuscular stimulation - Part I: Autoregressive modeling as a means of EMG signature discrimination,” *IEEE Transactions on Biomedical Engineering,* vol. 35, no. 4, pp. 230-237, 1988.

[32] L. A. Bernotas, P. E. Crago, and H. J. Chizeck, “A Discrete-Time Model of Electrcally Stimulated Muscle,” *IEEE Transactions on Biomedical Engineering,* vol. BME-33, no. 9, pp. 829 - 838, 1986.

[33] A. T. a. G. Moser, D., “Identification of nonstationary models with application to myoelectric signals for controlling electrical stimulation of paraplegics,” *IEEE Transactions on Acoustics, Speech and Signal Processing,* vol. 37, no. 5, pp. 713 - 719, 1989.

[34] S. Y. Kiryu T, and Ishioka K., “Investigation on parametric analysis of dynamic EMG signals by a muscle-structured simulation model.,” *IEEE Transactions on Biomedical Engineering,* vol. 39, no. 3, pp. 280-288, 1992.

[35] A. a. P. Del Boca, D.C., “Myoelectric signal recognition using fuzzy clustering and artificial neural networks in real time,” in 1994 IEEE International Conference on Neural Networks, 1994. IEEE World Congress on Computational Intelligence. , Orlando, FL , USA 1994, pp. 3098 - 3103.

[36] G. Cheron, J. P. Draye, M. Bourgeios *et al.*, “A dynamic neural network identification of electromyography and arm trajectory relationship during complex movements,” *IEEE Transactions on Biomedical Engineering,* vol. 43, no. 5, pp. 552-558, May. 1996.

[37] F. H. Y. Chan, Y. S. Yang, F. K. Lam *et al.*, “Fuzzy EMG classification for prosthesis control,” *IEEE Transactions on Rehabilitation Engineering,* vol. 8, no. 3, pp. 305-311, Sept. 2000.

[38] A. Belouchrani, Abed-Meraim, K., Amin, M.G., and Zoubir, A.M., "Joint anti-diagonalization for blind source separation." pp. 2789 - 2792.

[39] D. Farina, C. Fevotte, C. Doncarli *et al.*, “Blind separation of linear instantaneous mixtures of nonstationary surface myoelectric signals,” *IEEE Transactions on Biomedical Engineering,* vol. 51, no. 9, pp. 1555-1567, Sept. 2004.

[40] Y. M. Kanosue K, Akazawa K, and Fujii K., “The number of active motor units and their firing rates in voluntary contraction of human brachialis muscle.,” *Japan Journal of Physiology* vol. 29, no. 4, pp. 427-443, 1979.

[41] R. P., “Intra- and extracellular potential fields of active nerve and muscle fibres. A physico-mathematical analysis of different models.,” *Thrombosis et diathesis haemorrhagica. Supplementum.,* vol. 321, pp. 1-168, 1969.

[42] N. S. a. S. E., “Simulation of single muscle fibre action potentials.,” *Medical & Biological Engineering & Computing.,* vol. 21, no. 2, pp. 158-165, 1983.

[43] S. D. a. B. Nandedkar, P.E., “Phase interaction in the compound muscle act ion potential: application to motor unit estimates,” in IEE Colloquium on Neurological Signal Processing, London , UK 1992, pp. 4/1 - 4/5

[44] K. B. Englehart, and P. A. Parker, “Single Motor Unit Myoelectric Signal Analysis with Nonstationary Data,” *IEEE Transactions on Biomedical Engineering,* vol. 41, no. 2, pp. 168-180, Feb. 1994.

[45] Y. T. Zhang, Herzog, W., and Liu, M.M., “A mathematical model of myoelectric signals obtained during locomotion,” in IEEE 17th Annual Conference on Engineering in Medicine and Biology Society, 1995., Montreal, Que. , Canada 1995, pp. 1403 - 1404

[46] S. a. N. Karlsson, L., “Real-time system for EMG signal analysis of static and dynamic contractions,” in IEEE 17th Annual Conference on Engineering in Medicine and Biology Society, 1995., Montreal, Que. , Canada 1995, pp. 1347 - 1348.

[47] J. Duchene, and J. Y. Hogrel, “A model of EMG generation,” *IEEE Transactions on Biomedical Engineering,* vol. 47, no. 2, pp. 192-201, Feb. 2000.

[48] A. Hamilton-Wright, and D. W. Stashuk, “Physiologically based simulation of clinical EMG signals,” *IEEE Transactions on Biomedical Engineering,* vol. 52, no. 2, pp. 171-183, Feb. 2005.

[49] *S.* Bouisset, “*EMG and muscular force in normal motor activities*,” in 4th International Congress on EMG, Brussels, 1973.

[50] a. B. G. Perry J, “EMG-force relationships in skeletal muscle.,” *Critical Reviews in Biomedical Engineering,* vol. 7, no. 1, pp. 1-22, 1981.

[51] A. J. Fuglevand, D. A. Winter, and A. E. Patla, “Models of Recruitment and Rate Coding Organization in Motor-Unit Pools,” *Journal of Neurophysiology,* vol. 70, no. 6, pp. 2470-2488, Dec. 1993.

[52] A. Seth, and M. G. Pandy, “A neuromusculoskeletal tracking method for estimating individual muscle forces in human movement,” *Journal of Biomechanics,* vol. 40, no. 2, pp. 356-366, 2007.